

Bureau International des Poids et Mesures

Guide to Secondary Thermometry

Industrial Platinum Resistance Thermometers



Consultative Committee for Thermometry
under the auspices of the
International Committee for Weights and Measures

Contents

| | | |
|--------|--|----|
| 1. | Introduction | 5 |
| 2. | Working principles and construction | 6 |
| 2.1. | Resistance and resistivity..... | 6 |
| 2.2. | Construction | 7 |
| 2.2.1. | Wire-wound | 9 |
| 2.2.2. | Film types | 10 |
| 2.2.3. | High precision..... | 11 |
| 2.3. | Annealing | 12 |
| 2.4. | The Callendar-Van Dusen equation, national and international specifications..... | 12 |
| 2.4.1. | Tolerance bands | 14 |
| 2.4.2. | The Resistance-Temperature sensitivity | 16 |
| 2.5. | Selection guide..... | 17 |
| 2.5.1. | Accuracy | 18 |
| 2.5.2. | Temperature range | 19 |
| 2.5.3. | Environment..... | 19 |
| 2.5.4. | Construction..... | 19 |
| 2.5.5. | Sheathing..... | 20 |
| 3. | Instrumentation | 21 |
| 3.1. | Probe and connections | 21 |
| 3.1.1. | Lead resistance..... | 21 |
| 3.1.2. | Thermal emfs | 21 |
| 3.1.3. | Self-heating | 21 |
| 3.2. | Verification and calibration of resistance bridges | 21 |
| 3.2.1. | Zero and complement checks | 21 |
| 3.2.2. | The linearity check | 22 |
| 3.3. | Use of DC meters and industrial transmitters | 23 |
| 4. | Limitations in performance | 24 |
| 4.1. | Self-heating | 24 |
| 4.2. | Immersion..... | 26 |
| 4.3. | Response time | 28 |
| 4.4. | Lead resistance | 30 |
| 4.4.1. | Two-wire resistance measurement..... | 30 |
| 4.4.2. | Three-wire resistance measurement | 31 |

| | | |
|--------|--|----|
| 4.4.3. | Four-wire resistance measurement | 32 |
| 4.5. | Insulation resistance | 33 |
| 4.6. | Thermoelectric effects, DC and AC measurements | 35 |
| 4.6.1. | DC measurements | 35 |
| 4.6.2. | AC measurements | 36 |
| 4.7. | Hysteresis and short-term stability..... | 36 |
| 4.7.1. | Mechanical | 36 |
| 4.7.2. | Moisture | 38 |
| 4.7.3. | Oxidation | 39 |
| 4.7.4. | Characterisation of hysteresis..... | 40 |
| 4.7.5. | Specific hysteresis test procedures | 41 |
| 4.8. | Reproducibility, or long-term stability..... | 41 |
| 4.9. | Contamination | 47 |
| 4.10. | Electromagnetic interference | 48 |
| 5. | Calibration | 50 |
| 5.1. | Methods..... | 50 |
| 5.2. | Equations | 50 |
| 5.2.1. | Polynomial functions..... | 52 |
| 5.2.2. | CVD function | 52 |
| 5.2.3. | Direct use of the ITS-90 interpolation for IPRTs..... | 52 |
| 5.3. | Examples of processing IPRT calibration data, and uncertainties | 53 |
| 5.3.1. | Example of interpolation..... | 53 |
| 5.3.2. | Example 2: Calibration of a direct reading temperature indicator with two IPRT probes | 56 |
| 6. | Conclusions and further reading..... | 61 |
| 7. | Appendix 1: The original and modern Callendar-Van Dusen equations | 62 |
| 8. | References..... | 64 |

Last updated 22 November 2021

Guide on Secondary Thermometry

Industrial Platinum Resistance Thermometers

J V Pearce, National Physical Laboratory, United Kingdom
R L Rusby, National Physical Laboratory, United Kingdom
K Yamazawa, National Measurement Institute of Japan, Japan
S Rudtsch, Physikalisch-Technische Bundesanstalt, Germany
L Iacomini, Istituto Nazionale di Ricerca Metrologica, Italy
G Lopardo, Istituto Nazionale di Ricerca Metrologica, Italy
D R White, Measurement Standards Laboratory of New Zealand, New Zealand
W L Tew, National Institute for Standards and Technology, USA

ABSTRACT

This document is a part of guidelines, prepared by the Consultative Committee for Thermometry, on the techniques for approximating the International Temperature Scale of 1990.

It collates information on industrial platinum resistance thermometry. The information includes: working principles and construction; associated instrumentation; limitations in performance; and maintenance measures such as annealing and calibration procedures. Particular attention is given to typical performance and sources of uncertainties.

1. Introduction

Industrial platinum resistance thermometers (IPRTs) use platinum resistors (referred to here as sensors, elements, detectors, probes or simply IPRTs), which can withstand the conditions found in industrial processes. These conditions are likely to include mechanical and thermal shock, stress and vibration to varying degrees, and application at high pressures or in chemically hostile environments. The sensors or probes should also be small enough so they do not obstruct the process being monitored, and adapted as necessary for operation in air, other gases or vacuum, in liquids or on solid surfaces, in lightweight or heavy-duty conditions.

IPRTs are normally made to meet the specifications of international documentary standards organisations, most notably the IEC 60751 [IEC 60751], ASTM E1137 [ASTM E1137], or other harmonised or technically equivalent national standards. These apply over temperature ranges from $-200\text{ }^{\circ}\text{C}$ to $650\text{ }^{\circ}\text{C}$ or $850\text{ }^{\circ}\text{C}$, with tolerances specified over various temperature ranges between $-50\text{ }^{\circ}\text{C}$ and $650\text{ }^{\circ}\text{C}$ or $660\text{ }^{\circ}\text{C}$.

Two main types of IPRT resistor elements are made (see Section 2). Wire-wound types are constructed from platinum wires of a lower purity than that used in the Standard Platinum Resistance Thermometers (SPRTs) or in pure platinum thermoelements, sometimes referred to as ‘reference grade’ platinum. In film types the platinum is deposited on an alumina substrate, and the processing is engineered to achieve the required temperature coefficient. Thus, while the mechanisms responsible for the lower temperature coefficient are significantly different for film IPRTs than for wire-wound types (see Section 2.2), the resistance ratio $R(100\text{ }^{\circ}\text{C})/R(0\text{ }^{\circ}\text{C})$ of all IPRTs conforming with the IEC and ASTM specifications is about 1.385, compared with 1.3925 for SPRTs. It follows that IPRTs do not conform to the specifications of the ITS-90.

Although IPRTs do not generally achieve the reproducibility and accuracy of SPRTs, their performance is nevertheless significantly (a factor of 10 or more) better than thermocouples in industrial environments up to about $600\text{ }^{\circ}\text{C}$. For this reason, many millions are used across the whole spectrum of science, technology, engineering and manufacturing industry. IPRTs have almost entirely replaced precision liquid-in-glass thermometers as laboratory references.

Commercial IPRT sensors (such as ‘Pt100’ designations for sensors of nominally $100\ \Omega$ at $0\text{ }^{\circ}\text{C}$) are readily available in a wide range of designs or configurations to achieve the required performance at relatively low cost. If the manufacturing tolerances ($0.1\text{ }^{\circ}\text{C}$ to $0.6\text{ }^{\circ}\text{C}$ at $0\text{ }^{\circ}\text{C}$, see Section 2.4) are not small enough, the assembled thermometers can be calibrated to obtain accuracies (approximations to the ITS-90) within $\pm 0.05\text{ }^{\circ}\text{C}$ between $-80\text{ }^{\circ}\text{C}$ and $450\text{ }^{\circ}\text{C}$ or even $660\text{ }^{\circ}\text{C}$, and within $\pm 0.01\text{ }^{\circ}\text{C}$ between $-40\text{ }^{\circ}\text{C}$ and $100\text{ }^{\circ}\text{C}$.

The lower limit of $-200\text{ }^{\circ}\text{C}$ includes the temperatures encountered in industries concerned with bulk transport, storage and usage of liquid natural gas and air. The upper limit is the maximum at which it may be possible to use IPRTs and is limited by physical and chemical changes induced in the platinum, often due to strain and contamination by the supporting material and sheath. Common upper limits for commercial IPRTs are $250\text{ }^{\circ}\text{C}$ or $450\text{ }^{\circ}\text{C}$, where a wider range of constructional

materials can be used and lower uncertainties can be achieved; the range is most often determined by the sheath, interconnections and insulations.

This document describes the different types and designs of IPRTs, the instrumentation used with them, guidance on calibration and use, and the various sources of error, and key references. Examples of calibration equations and certificates are given in the appendices. Recommended texts for further reading include Nicholas and White [Nicholas 2001], Michalski, Eckersdorf, Kucharski and McGhee [Michalski 2001], and Childs [Childs 2001].

2. Working principles and construction

Before discussing the construction of sensors in more detail, in Section 2.2, it is useful to review how the manufacturing processes may affect the resistance characteristics.

2.1. Resistance and resistivity

The resistance, R , of a wire of a given material (metal) increases with the length of the wire and decreases with the cross-sectional area. The specific resistance, or resistivity, ρ , is the resistance normalised to unit dimensions. For a wire of length l / m and cross-sectional area A / m² we have $\rho = RA/l$ in units of Ω m (in practice it is usually given in units of n Ω m). Unlike the resistance, the resistivity is a characteristic property of the metal, being the same, or closely similar, for all (pure) samples.

As the temperature increases, the atoms in the lattice vibrate more strongly, and the electrons carrying an electric current are more vigorously scattered. As a result, the resistivity of the metal increases approximately in proportion to the absolute temperature. The resistivity of platinum has small quadratic and higher-order components, which lead to a slowly decreasing temperature coefficient (and hence sensitivity) over a wide temperature range. This behaviour, together with the availability of pure inert metals with enough ductility so that fine wires can be drawn, is what makes them attractive as sensors for thermometry. Platinum has been the preferred choice from the origins of resistance thermometry in the late nineteenth century, because it is chemically quite inert and has good physical properties, and has a comparatively high resistivity, $\sim 9.8 \cdot 10^{-8} \Omega$ m at 0 °C (about six times that of copper), with a relative sensitivity, dR/Rdt , of $\sim 0.004 / ^\circ\text{C}$ (comparable with that of copper), and can operate over an extremely wide temperature range.

SPRTs are made with very pure well-annealed platinum, but wire-based IPRTs are made with platinum that is deliberately doped with other noble metal impurities in order to make the wires less soft and the coils easier to form and manipulate. In film types the platinum is in a partially disordered state. Thus, in both cases the resistivity includes a significant contribution from the scattering of electrons by impurity atoms and defects (dislocations, vacancies, grain boundaries, etc.) in the crystal lattice. To a first order approximation, the various mechanisms operate independently, and the additional resistivities are independent of temperature. As a

result, the resistivities caused by them are broadly additive and constant. This approximation is known as Matthiessen's rule¹, which gives the total resistivity as a sum of individual components:

$$\rho_{\text{tot}}(t) = \rho_t(t) + \rho_i + \rho_d \quad (2.1.1)$$

where the total resistivity $\rho_{\text{tot}}(t)$ is expressed as the sum of components due to the lattice vibrations $\rho_t(t)$, impurities ρ_i , and other crystal defects ρ_d . The last two are small compared with the first, but because they are approximately independent of temperature they have the effect of reducing the sensitivity of IPRTs compared with SPRTs.

This can be seen by considering the resistance ratios $R(t)/R(0\text{ °C})$, which are essentially resistivity ratios (to the extent that the ratio A/l is constant, i.e. if the expansivity of platinum is ignored). Thus we can write:

$$\frac{R(t)}{R(0\text{ °C})} \approx \frac{\rho_{\text{tot}}(t)}{\rho_{\text{tot}}(0\text{ °C})} \approx \frac{\rho_t(t) + \rho_i + \rho_d}{\rho_t(0\text{ °C}) + \rho_i + \rho_d} \quad (2.1.2)$$

The constant terms, ρ_i and ρ_d , are a smaller proportion of $\rho_t(t)$ than they are of $\rho_t(0\text{ °C})$, for $t > 0\text{ °C}$, so they have the effect of reducing $R(t)/R(0\text{ °C})$ below its ideal value. (Conversely, for $t < 0\text{ °C}$, $R(t)/R(0\text{ °C})$ is higher than its ideal value.) Their effect is greater for IPRTs than for SPRTs because the constant terms are larger, and the effect is therefore to reduce the sensitivity dR/dt further below its ideal value. Consequently, $R(100\text{ °C})/R(0\text{ °C})$ is typically ~ 1.3851 for IPRTs, compared with > 1.3925 for SPRTs.

For historical reasons, the parameter used to characterise an IPRT is α , the average normalised temperature coefficient between 0 °C and 100 °C :

$$\alpha = \frac{R(100\text{ °C}) - R(0\text{ °C})}{R(0\text{ °C}) \cdot 100\text{ °C}} \quad (2.1.3)$$

Hence, if $R(100\text{ °C})/R(0\text{ °C})$ is ~ 1.3851 , $\alpha \sim 0.003851\text{ °C}^{-1}$. A higher purity yields a higher value of α .

2.2. Construction

IPRTs manufactured to withstand the rigours of industrial use require the platinum resistance element to be firmly supported. They may be wire-wound or film-type (see Section 2.2.1 and 2.2.2 for more details):

- Wire-wound:
 - With a bifilar platinum wire winding fused onto a glass or alumina former, and a resistance adjusted to a nominal value by trimming the

¹ Matthiessen's approximation is qualitatively useful, but not quantitatively reliable. In particular, it is well known to break down at temperatures below -200 °C .

- length of the winding, and a sleeve or glass coating over the assembly, the whole element being fused together (see Figure 2.2.1, centre).
- With a platinum coil partially supported in the bores of a 2- or 4-bore ceramic tube; the remaining space is filled with alumina powder, or a glass frit is used, to fix the coils and improve heat transfer. Both ends are then closed with a ceramic sealing compound (see Figure 2.2.1, left).
- With platinum foil: a winding of platinum is embedded between two self-adhesive polyimide sheets, with two nickel tapes emerging for the electrical connection. These are semi-flexible and designed for surface temperature measurements.
- Film-type, in which the platinum is deposited on a ceramic substrate and laser-cut or etched to form a resistance grid (see Figure 2.2.1, right).
 - In a ‘thick-film’ sensor the platinum is screen-printed as a layer of several 10s of micrometres thickness, starting from a thixotropic metal/binder paste. It is then heat-treated to achieve the required temperature coefficient, leads are attached and a protective coating is applied.
 - In a ‘thin-film’ sensor the platinum is deposited by sputtering from a pure Pt target onto a high purity alumina substrate, often to a film thickness of about 1 μm . After laser-cutting to form a resistance grid pattern, it is heat treated and coated with protective covering and passivation layers. Other thin-film PRT technologies use altered compositions in the substrates and reduced film thicknesses.

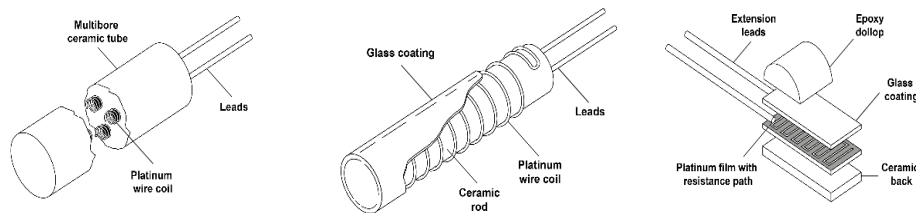


Figure 2.2.1. Typical designs of IPRT sensing element: partially- and fully-supported wire-wound (left and centre), and film (right).

These designs render the sensors extremely robust, but at the same time they reduce the stability of the resistance: there is always a compromise between accuracy and robustness. There are three main reasons for this. The first is that, on thermal cycling, differences between the thermal expansion coefficient of the platinum and that of the embedding matrix leads to extra strain in the wire, and plastic deformation, which cause changes in resistance. While some strain can be annealed out at sufficiently high temperatures, irreversible dimensional changes cannot. The second reason is that at high temperatures, changes in resistance occur because of

contamination of the platinum due to diffusion of impurities from the surrounding materials, especially the metal protective sheath. Lastly, in partially supported elements vibration and shock cause flexing of the wire, work hardening and an increase in resistance. This can be annealed out in thermometers made for use up to 400 °C.

Different designs achieve different levels of compromise. Partially supported sensors allow some differential expansion and they are often used in laboratory standard IPRTs because they may achieve low hysteresis (a few millikelvin over limited ranges) and generally more repeatable performance. Fully supported wire-wound IPRTs are more robust but allow little expansion and hence may suffer from greater instability and hysteresis. In film-type sensors the film expands and contracts with the substrate, leading to slightly different characteristics, but the hysteresis may be low.

The documentary standards referred to specify type-tests for the various designs and routine tests for individual sensors, which manufacturers must undertake in order to qualify their production for sale. These include mechanical (e.g. vibration), thermal (temperature ageing, cycling, hysteresis, etc) and electrical (resistance values, insulation resistance) tests. Purchasers with particular requirements are advised to undertake their own tests to verify that the sensors are likely to meet these requirements.

The size of sensing element typically ranges from about 1 mm² for some thin film types to about 4.5 mm diameter x 30 mm for wire-wound types. The wire-wound types typically utilise platinum wire of diameters between about 20 µm to 50 µm. In contrast, most film IPRTs are made from films approximately 1 µm in thickness. The designs are now considered in more detail.

2.2.1. *Wire-wound*

A wide variety of techniques have been devised for winding the platinum wire [Actis 1982, Bass 1980, Connolly 1982]. The configuration offering the best stability [Actis 1982] and the lowest hysteresis [Curtis 1982] is that in which a platinum coil is partially supported inside the capillaries of a twin- (or four-) bore, high purity alumina insulator, typically about 3 mm in outside diameter by 15 to 25 mm long. Either the use of a cement or glass frit to fix one side of the coil to the capillary wall or, preferably, the insertion of soft alumina powder, prevents the platinum coil from vibrating freely and helps in achieving good reproducibility in industrial applications. Two wires emerge, to which additional leads can be connected. This design is illustrated in the left panel of Figure 2.2.1. By these techniques, it is possible to construct thermometers with good mechanical properties and $R(0\text{ °C})$ stabilities of a few hundredths of a degree when used over the range -200 °C to 660 °C.

For applications where vibration levels are high, the platinum wire is best wound upon a glass or ceramic rod which is then coated with glass or ceramic cement, as shown in Figure 2.2.1 (centre). The glass or ceramic is selected to match the expansion properties of the platinum. The resistor is extremely robust, but it has

somewhat poorer stability and greater hysteresis than with a less rigidly supported coil, and it is only suitable for use over a limited temperature range.

Thermometers (or probes) are often assembled with three or four (preferably platinum) leads in an insulated stainless steel or Inconel sheath, with diameters ranging from 1 mm to 6 or 7 mm and up to 450 mm long or more, with a head for handling and an epoxy feed-through, from which a cable connects it to the measuring instrumentation. Heavy-duty industrial sensors are often connected to a ceramic terminal block in a protective steel cover, from which cables connect to a process control centre.

Another sensor type, best suited to surface temperature measurements, is made with a winding of platinum foil embedded between two self-adhesive polyimide sheets, with two nickel tapes emerging for the electrical connection.

2.2.2. *Film types*

Advances in recent decades have led to the development of IPRTs having a platinum film as the sensing element, rather than a platinum wire. The platinum is deposited onto ceramic wafers (by screen printing or vapour deposition) and etched or laser-cut in a variety of geometries (Figure 2.2.1, right panel), including the frequently used sensor of 3 mm diameter by 25 mm long. They are manufactured to conform to the national and international standard specifications, with some qualifications.

One advantage of film sensors is that they are less susceptible to mechanical shock and so are more rugged than conventional wire-wound detectors. They may also have low hysteresis for temperatures less than about 250 °C (to avoid annealing) because the platinum is bonded to the substrate and expands and contracts with it. This also means the strain is an integral part of the sensor response, which results in subtle differences in the response when compared to wire-wound types and reduces the tolerance temperature ranges for film-type PRTs (see Section 2.4.1).

These sensors have a performance almost equal to that of the glass coated wire wound sensors over the range from cryogenic temperatures up to 500 °C, and since their production can be partly automated, they are much cheaper to produce. They have a fast response, due to the intimate contact of the film with the substrate and the surroundings, and their lower mass. They are particularly suited to applications such as surface temperature measurement. However, they may be less repeatable on temperature cycling, due to plastic deformation, and are less suitable for use at temperatures much above 300 °C.

Thin-film platinum resistor elements are fabricated using a process similar to those in the semiconductor industry. A platinum layer, up to ~1 µm, is deposited onto an aluminium oxide substrate. The platinum layer is then structured using photolithography techniques. After the addition of a protective glass layer, the resistance is adjusted to the required value by laser trimming. Until relatively recently, many thin-film sensors have not demonstrated adequate long-term stability at higher temperatures. In harsh industrial conditions, contamination of the platinum layer by other constituents of the probe has been problematic, causing corresponding changes in the resistance versus temperature characteristic. A second

limitation has been the difficulty in ensuring the characteristic complies with the tolerances specified by IEC 60751 [IEC 60751]; in general, the tolerance can only be complied with over a limited temperature range.

The platinum in the film is partially disordered, but there is a correlation between sputtering time (i.e. thickness) and the disorder [Zhang 1997], which allows the manufacturer to engineer samples with the required temperature coefficient (note that it is the film structure, and hence ρ_d in Eq. (2.1.1), which is principally responsible for the reduced temperature coefficient, rather than the impurities, ρ_i , as in wire-wound types).

In more recent developments, the substrate composition has been altered to raise its temperature coefficient of expansion to something closer to that of Pt [Kretz 2013]. The smaller mismatch in expansion allows the platinum film to better match the curve for bulk wire, and the required film thickness is reduced to a few hundred nanometers. In addition, there may be some deliberate doping of the Pt, so the sputtering targets need no longer be as pure as they are in the older technology.

These new production technologies have brought about clear improvements, and measurements suggest that the newer thin-film IPRTs, although initially exhibiting a larger spread of individual sensor characteristics than seen within a given batch or type, are otherwise comparable to wire-wound IPRTs [Boguhn 2011].

2.2.3. High precision

There are some approaches to combine fabrication techniques of SPRTs and IPRTs to yield high precision temperature sensors. For example, for use up to the gold point (1064 °C), the sensor is formed by many short platinum wires, embedded in the holes of an alumina insulator and welded together in series (the ‘birdcage’ design) [Curtis 1982]. Two types of sensor with 5 Ω or 3 Ω resistance at 0 °C have been designed, as shown in Figure 2.2.2.

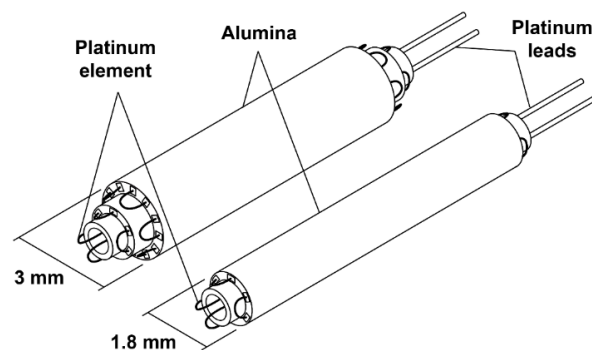


Figure 2.2.2. Construction of the ‘birdcage’ sensing element of IPRTs up to the gold point [Arai 1992].

Using platinum wire of 0.11 mm diameter, 30-bore alumina tubes were used to support the element for the 5 Ω type, and 14-bore alumina tubes were used for the 3 Ω type. The structure is suitable for use in either a horizontal position or a vertical position. The sensor with four platinum leads, insulated by a four-bore alumina tube, is encased in a quartz tube, or an alumina tube, that is sealed with epoxy resin at the top after being filled with an atmosphere of dry air. The sensors were initially annealed at 1200 °C for at least 40 hours after fabrication.

Another approach is the use of high purity platinum wires for wire wound sensors with miniature structures and yielding a high resistance ratio comparable to SPRTs [Yamazawa 2011]. In [Yamazawa 2011], a small sized PRT is packed inside a 0.8 mm diameter, 8 mm length alumina insulator, and their characteristics evaluated up to 156 °C.

2.3. Annealing

Annealing is the most effective way of reducing internal strain of the sensing element caused by thermal cycling and the cold working introduced by manufacture and vibrations or shocks. Annealing involves exposure of the sensing element and nearby region of the probe to a temperature slightly higher than the expected maximum temperature of use for several hours, which introduces a high degree of mobility to the constituent atoms and enables them to find their equilibrium, strain-free, positions. It also has the benefit of ‘resetting’ the oxidation state of the platinum, which can be responsible for hysteresis effects. Manufacturers of platinum resistor elements subject the elements to high temperature annealing after the cold working is completed and prior to being installed into sheaths. This annealing process is empirically derived to restore the α value for the element so that it is suitable for use in the finished IPRT and conforms to the appropriate tolerance band specification.

For most probes, made for temperatures below 250 °C, annealing is generally not worthwhile, but for probes made for use above this temperature, annealing may have some benefit by improving stability and hysteresis characteristics. The probe must be designed for exposure to these higher temperatures, otherwise there is a risk of contamination. Such probes are more expensive than the usual IPRT probes.

Related to annealing is thermal cycling. In general, hysteresis is caused by reversible changes in resistance from annealed to strained conditions in the platinum (at least in the temperature range where hysteresis due to reversible oxidation of the platinum can also occur). This means that the IPRT should be cycled over the intended temperature range of use and, subsequently, thermal cycling should not exceed the limits of this stabilization thermal cycle.

2.4. The Callendar-Van Dusen equation, national and international specifications

Various standardization organisations, including the International Electrotechnical Commission (IEC), all the European national electrotechnical committees of CENELEC, and the American Society for Testing and Materials (ASTM), among others, have promulgated technically equivalent specifications for IPRTs with

$R(100\text{ °C}) / R(0\text{ °C}) = 1.3851$ [IEC 60751, ASTM E1137]². This specifies the temperature coefficient and tolerances of IPRTs complying with the standard, but the value of $R(0\text{ °C})$ is not specified. Most commonly, for sensors designated Pt100s, $R(0\text{ °C})$ is $100\ \Omega$, but higher values, $500\ \Omega$, $1000\ \Omega$ or even more, are available: these provide greater measurement sensitivity, though they may be more fragile and less reliable in service. These are nominal values that are accurate to within some manufacturing tolerance. In practice, the actual value for $R(0\text{ °C})$ is almost always determined by the end user through use of an Ice Melting Point (IMP or ‘Ice Point’) [ASTM E563].

The relationship between R and t_{90} is generated from the Callendar-Van Dusen (CVD) equations (see also Appendix 1):

$$\frac{R(t_{90})}{R(0^{\circ}\text{C})} = 1 + A t_{90} + B t_{90}^2 \quad t_{90} \geq 0\text{ °C} \quad (2.4.1)$$

and

$$\frac{R(t_{90})}{R(0^{\circ}\text{C})} = 1 + A t_{90} + B t_{90}^2 + C t_{90}^3 (t_{90} - 100\text{ °C}) \quad t_{90} < 0\text{ °C} \quad (2.4.2)$$

where the coefficients are given in Table 2.4.1.

Table 2.4.1. Standard coefficients of the CVD equation.

| Constants | Values |
|-----------|--|
| A | $3.9083 \cdot 10^{-3}\text{ °C}^{-1}$ |
| B | $-5.775 \cdot 10^{-7}\text{ °C}^{-2}$ |
| C | $-4.183 \cdot 10^{-12}\text{ °C}^{-4}$ |

IEC and CENELEC specify for Equation (2.4.1) the range 0 °C to 850 °C , while ASTM limits the range to 0 °C to 650 °C . The lower limit of Equation 2.4.2 is -200 °C .

Some standards exist for other grades of IPRT. For example, the International Organization of Legal Metrology (OIML) has published an International

² Although the CVD equation is written in terms of the ratio of resistances $R(t)/R(0\text{ °C})$, the standards continue to specify IPRT sensors using the alpha coefficient as formerly used (see Appendix 1), where

$$\alpha = R(100\text{ °C}) - R(0\text{ °C}) / (100 R(0\text{ °C}))$$

or

$$\alpha = (R(100\text{ °C})/R(0\text{ °C}) - 1) / 100\text{ °C}$$

This is the mean normalised temperature coefficient of the resistance in the interval 0 °C to 100 °C and, in this case, α takes the value 0.003581 °C^{-1} .

Recommendation³, R 84 (2003), for IPRTs with $R(100\text{ °C})/R(0\text{ °C}) = 1.385$ and 1.391 . PRTs with $R(100\text{ °C})/R(0\text{ °C}) = 1.3916$, have been made to a Japanese specification, the JIS C 1604-1981[JIS 1981]. These are often referred to as ‘JPt100’ and although they are no longer standardised, a newer version may be available with $R(100\text{ °C})/R(0\text{ °C}) = 1.3920$ [Sakurai 1996].

2.4.1. Tolerance bands

A significant component to the International Standard Specifications of IPRTs are the so-called ‘tolerance bands’, which define the accuracy performance for ‘off-the-shelf’ (i.e. uncalibrated) IPRTs over specific temperature ranges. For IEC 60751 [IEC 60751] the standard segregates the accuracy performance into a number of defined tolerance ‘classes’. For the ASTM E1137 [ASTM E1137] the accuracy performance is segregated into two tolerance ‘grades’. While the nominal resistance-temperature curve for IEC 60751 is equivalent to that of ASTM E1137, the tolerance classes and tolerance grades are not equivalent, and a Class B IPRT under the IEC specification is not the same as a Grade B IPRT under the ASTM specification.

The 2008 version of IEC 60751 ed. 2 (2008) [IEC 60751] specifies tolerance classes and temperature ranges for resistors (sensors) and thermometers. The temperature ranges of validity also differ for different sensor structures (i.e. wire wound or film resistors). Tables 2.4.2 and 2.4.3 show the tolerance classes defined by IEC 60751 ed. 2 (2008). The specified tolerances of the IEC standards are also shown in Figure 2.4.1. Note that many manufacturers supply elements with reduced tolerance bands; for example, a 1/10th DIN specification refers to a tolerance of 1/10th on the R_0 value only.

Table 2.4.2. Tolerances for resistors in IEC 60751 ed. 2 (2008).

| <i>For wire wound resistors</i> | | <i>For film resistors</i> | | Tolerance value ^a °C |
|---------------------------------|-------------------------------------|---------------------------|-------------------------------------|------------------------------------|
| Tolerance class | Temperature range of validity °C | Tolerance class | Temperature range of validity °C | |
| W 0.1 | -100 to +350 | F 0.1 | 0 to +150 | $\pm(0.1 + 0.0017 t)$ |
| W 0.15 | -100 to +450 | F 0.15 | -30 to +300 | $\pm(0.15 + 0.002 t)$ |
| W 0.3 | -196 to +660 | F 0.3 | -50 to +500 | $\pm(0.3 + 0.005 t)$ |
| W 0.6 | -196 to +660 | F 0.6 | -50 to +600 | $\pm(0.6 + 0.01 t)$ |

^a $|t|$ = modulus of temperature in °C without regard to sign.

Table 2.4.3. Tolerances for thermometers in IEC 60751 ed. 2 (2008).

| Tolerance class | Temperature range of validity °C | | Tolerance value ^a °C |
|-----------------|-------------------------------------|----------------|------------------------------------|
| | Wire wound resistors | Film resistors | |
| AA | -50 to +250 | 0 to +150 | $\pm(0.1 + 0.0017 t)$ |
| A | -100 to +450 | -30 to +300 | $\pm(0.15 + 0.002 t)$ |
| B | -196 to +600 | -50 to +500 | $\pm(0.3 + 0.005 t)$ |
| C | -196 to +600 | -50 to +600 | $\pm(0.6 + 0.01 t)$ |

³ OIML R 84 [OIML R 84] also specifies functions for copper and nickel resistance thermometers.

^a $|t|$ = modulus of temperature in °C without regard to sign.

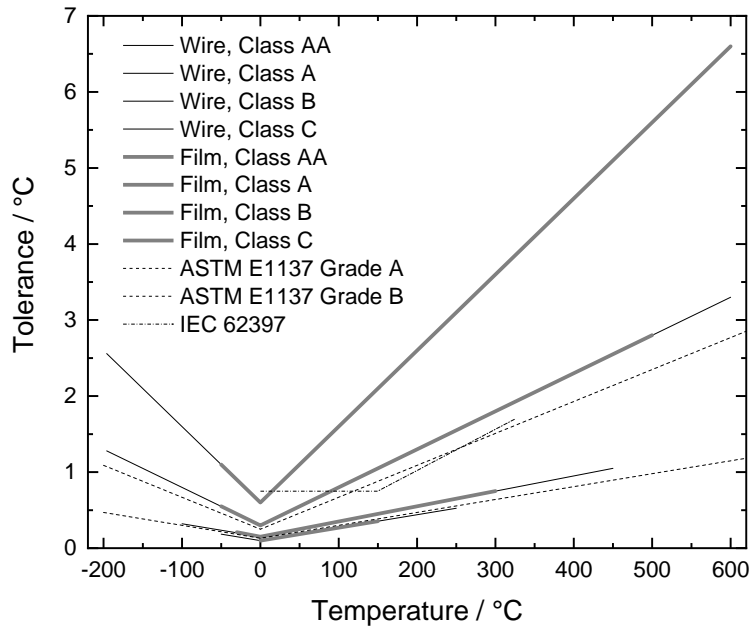


Figure 2.4.1. Tolerances for IPRTs as specified by IEC 60751 (2008) [IEC 60751], except where otherwise stated. To achieve lower uncertainties, calibration of the individual sensor is required.

The ASTM E1137 [ASTM E1137] standard specification defines two tolerance bands, referred to as Grades A and B. The ASTM E1137 specification does not make distinctions between wire and film resistors. The tolerance grade specifications are shown in Table 2.4.4 and are applicable to finished thermometers. Figure 2.4.1 shows all the film and wire-based IPRT tolerance bands for IEC and ASTM specifications.

Table 2.4.4. Tolerances for thermometers in ASTM E1137.

| Tolerance Grade | Temperature range of validity °C | Tolerance value ^a °C |
|-----------------|----------------------------------|---------------------------------|
| A | -200 to +650 | $\pm(0.13 + 0.0017 t)$ |
| B | -200 to +650 | $\pm(0.25 + 0.0042 t)$ |

^a $|t|$ = modulus of temperature in °C without regard to sign.

There is also an IEC standard for IPRTs used in the safety systems of nuclear power plants [IEC 62397]. In this case the resistance-temperature curve is of the same form as that of IEC 60751 and ASTM E1137, but the *A* and *B* values are left unspecified. The single tolerance band limits are somewhat more relaxed below 100 °C (i.e. ± 0.75 °C) but otherwise similar to ASTM E1137 Grade B above 200 °C.

Boguhn [Boguhn 2011] has shown that commercially available thin-film IPRTs are not fully conforming to the Class A tolerance of the IEC 60751 standard in at least parts of the temperature range from $-50\text{ }^{\circ}\text{C}$ to $660\text{ }^{\circ}\text{C}$. In practice, the traditional film-type IPRTs are designed to yield an α value that conforms to the standards in so much as the specification $\alpha = A + 100B = 0.003851$ is satisfied. But the film IPRTs tend to yield different values for A and B than do the wire types, and so follow a slightly different curve, which limits the temperature range over which they can conform to the tolerance specification. However, in that same study it was also shown that a newer type of ‘optimised’ thin-film IPRT was able to conform with the Class A tolerance, illustrating the rapid pace of improvement of thin-film resistors in general.

2.4.2. The Resistance-Temperature sensitivity

Figure 2.4.2 shows how the resistance of an IPRT of $100\ \Omega$ at $0\text{ }^{\circ}\text{C}$ changes with temperature. The resistance increases almost linearly as the temperature increases, with a gradual decrease in the slope: thus, the sensitivity of approximately $0.4\ \Omega/^{\circ}\text{C}$ at $0\text{ }^{\circ}\text{C}$ decreases to about $0.3\ \Omega/^{\circ}\text{C}$ at $850\text{ }^{\circ}\text{C}$.

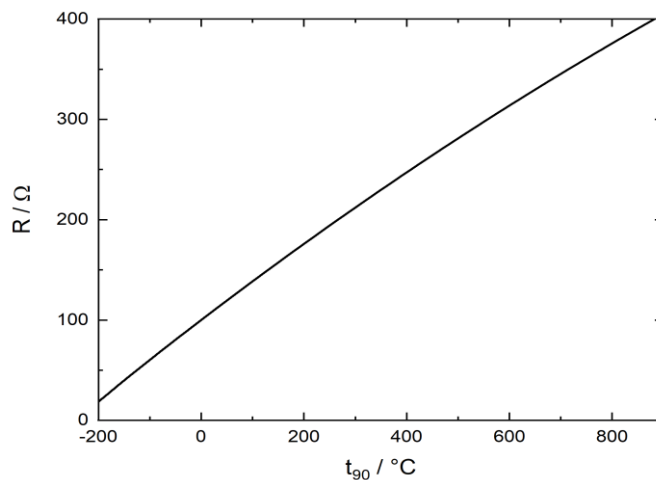


Figure 2.4.2. Resistance of an IPRT of $100\ \Omega$ at $0\text{ }^{\circ}\text{C}$ versus temperature.

Table 2.4.5 gives in Column 2 the resistances at a set of nine temperatures between $-200\text{ }^{\circ}\text{C}$ and $850\text{ }^{\circ}\text{C}$, according to IEC 60751, for a Pt resistor of $100\ \Omega$ at $0\text{ }^{\circ}\text{C}$. Columns 3 and 4 give sensitivities dR/dt in $\Omega/^{\circ}\text{C}$ or the inverse, which can be used to convert changes (errors or uncertainties) in resistance to the equivalent changes in temperature, and vice versa. Columns 5 to 8 do the same for the relative sensitivities F in $\% \text{ K}^{-1}$ and ppm (parts per million) of resistance per millikelvin of temperature change. These are useful for converting errors or uncertainties which are given in ppm, for example, in correcting reference resistance values for changes in temperature. It is sometimes also useful to utilise the logarithmic sensitivity, or $S = d\ln R/d\ln T$. For IPRTs close to $T = 300\text{ K}$, $S = TF \approx 1.0$, so that a $0.01\ \%$ uncertainty in R corresponds to a $0.01\ \%$ uncertainty in T .

Table 2.4.5. Values of resistance and sensitivity factors for IPRTs of 100 Ω at 0 $^{\circ}\text{C}$, between -200 $^{\circ}\text{C}$ and 850 $^{\circ}\text{C}$ according to IEC 60751.

| t_{90} $^{\circ}\text{C}$ | $R(t_{90})$ Ω | S'tivity dR/dt Ω / K | Inverse dt/dR K / Ω | Relative sensitivity % or ppm of R | | T equiv't 1% in R K | T equiv't 1 ppm in R mK |
|--------------------------------|-------------------------|--|---|---|----------------|-----------------------------|---------------------------------|
| | | | | % / K | ppm / mK | | |
| -200 | 18.520 | 0.432 | 2.31 | 2.33 | 23.34 | 0.43 | 0.043 |
| -100 | 60.256 | 0.405 | 2.47 | 0.67 | 6.73 | 1.49 | 0.149 |
| 0 | 100.000 | 0.391 | 2.56 | 0.39 | 3.91 | 2.56 | 0.256 |
| 100 | 138.506 | 0.379 | 2.64 | 0.27 | 2.74 | 3.65 | 0.365 |
| 200 | 175.856 | 0.368 | 2.72 | 0.21 | 2.09 | 4.78 | 0.478 |
| 400 | 247.092 | 0.345 | 2.90 | 0.14 | 1.39 | 7.17 | 0.717 |
| 650 | 329.640 | 0.316 | 3.17 | 0.10 | 0.96 | 10.44 | 1.044 |
| 850 | 390.481 | 0.293 | 3.42 | 0.07 | 0.75 | 13.34 | 1.334 |
| | | | | $100 \cdot F$ | $1000 \cdot F$ | | |
| | | | | $F = (1/R) (dR/dt)$ | | | |

2.5. Selection guide

While a significant number of manufacturers are producing platinum elements, many more firms in countries all over the world are assembling elements within sheaths for any type of application. Assembly of a platinum element in its sheath requires a factory or laboratory capability to conserve the original purity of all components, in order not to contaminate the platinum sensor when exposed to high operating temperature. Moisture must also be excluded in order to avoid leakage resistance and dielectric errors in the measurements.

For the selection of the platinum resistance element mounted (or to be mounted) within a complete IPRT, both the specific application and temperature range is to be considered, since, as previously described, many different types of IPRTs are available to satisfy different industrial applications. It is rarely the ultimate in reproducibility that is demanded but, rather, a modest reproducibility combined with good long-term stability under adverse conditions such as vibration, pressure, thermal cycling or corrosive atmosphere, together with interchangeability between thermometers made to the same specification. It is because of these requirements that an important selection is between robustness combined with interchangeability, and reproducibility.

For temperatures above 200 $^{\circ}\text{C}$ the limitations of IPRT stability begin to affect their suitability, especially if they are subject to regular cycling. Figure 2.5.1 summarises the best temperature range and accuracy that can be expected from the main types of PRT.

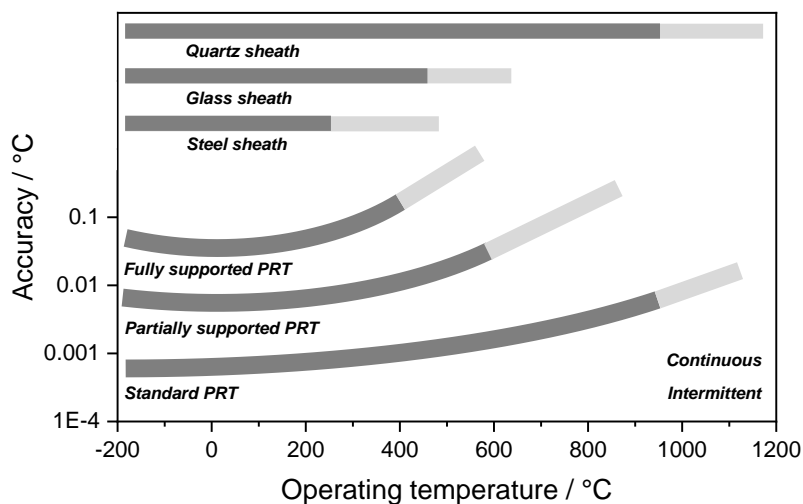


Figure 2.5.1. Approximate accuracy and range that can be achieved with the various types of PRT (after [Nicholas 2001, p239]). The top three horizontal bars illustrate the temperature ranges of different sheath materials.

There are five main factors to consider in the choice of industrial platinum thermometers [Nicholas 2001, pp 239-240]. These are itemised as follows.

2.5.1. Accuracy

For an uncalibrated IPRT, the accuracy is determined by the tolerance specification for which the IPRT is designed to conform. The tolerance bands described in Section 2.4.1 are widely recognised by manufacturers of IPRTs and are readily available. In contrast, for a calibrated PRT the accuracy can range anywhere from ± 0.001 °C to ± 1 °C, depending on the construction and required temperature range. In general, as the accuracy improves, so does the cost of the sensor or probe and the measurement instrumentation. The calibration accuracy of IPRTs is also strongly dependent on the temperature range and should be commensurate with the tolerance class to which they were originally manufactured. Typically, the accuracy may be < 0.1 % of the range for fully supported PRTs (glass-coated wires and film types, Figure 2.2.1) and < 0.005 % for partially supported PRTs (coils inserted into alumina tubes, Figure 2.2.1, left panel). To stabilise the sensors, or reduce the risk of instability, PRTs can be pre-tested by cycling them between the upper and lower limits of the range of use. Measurements at an intermediate temperature can usefully show the magnitude of any hysteresis. The best partially supported PRTs have hysteresis of less than 0.0002 % of the temperature range.

From the resistance measurement standpoint, choices will range from simple unipolar DC instruments (e.g. multimeters), to various bipolar DC instruments and AC resistance bridge instruments. The DC unipolar types are suitable for accuracies between ± 0.02 °C and ± 1 °C. AC bridges or switched DC systems are necessary to achieve accuracy better than ± 0.02 °C (see section 3.3).

2.5.2. *Temperature range*

As the temperature range increases, the demands on the quality of the environment and sheath increase. Above 250 °C, the environment must be free of contaminants. In general, partially supported ceramic elements in stainless steel sheaths are suitable, and fully supported elements should be suitable if the temperature is not regularly cycled. Above 450 °C, the platinum coils should be at most partially supported and silica (quartz) or alumina sheaths are required. IPRTs have a limited life at these temperatures, because of fatigue, contamination or failure of the connections. Above 650 °C, only some of the best partially supported PRTs will survive intermittent use to 850 °C, and the best uncertainties are likely to be 0.5 °C to 1 °C. To obtain the best performance, one strategy is to restrict the temperature range of use, so for example one PRT per 200 °C of range will extend the lifetime of the assembly.

2.5.3. *Environment*

The main considerations for the environment are vibration and mechanical shock. If either of these are a factor, fully supported elements should be used. Partially supported elements may be suitable if the vibration is small or if the assembly can be mechanically decoupled from the vibration. In a wet or humid environment, glass-coated elements should be used, and the assembly should be sheathed, to prevent excessive leakage current and moisture-induced hysteresis. In hostile or corrosive environments, again, the whole assembly (PRT element and leads structure) must be protected by a sheath, of stainless steel or other suitable material. If the IPRT is to measure the temperature inside a pressure vessel, it must be inserted into a permanently installed thermowell so it can be removed for maintenance. This further de-couples the sensor from the process, so it is likely to respond slowly (time-constants may be a minute or two, with consequences for the process control), and immersion characteristics may be poor.

2.5.4. *Construction*

Since sheathing is required for most applications, and the differential expansion of the sheath and lead wires greatly complicates assembly, elements should be purchased sheathed. A great deal of experience and proprietary information is needed to successfully construct an IPRT.

For laboratory applications a good quality PRT is partially supported, has four leads, and a hermetic seal in the head (also referred to as an ‘End Seal’ or a ‘Cold Seal’), where the leads emerge from the sheath and are connected to the external cable. A braided screen is needed for the cable; this screen should be connected to the sheath if it is metal. PTFE insulation should be used since it exhibits less AC loss and can withstand temperatures up to 200 °C.

2.5.5. *Sheathing*

The temperature range of the thermometer is determined to a large part by the choice of sheath. There are two types of sheathing material: metallic (e.g. stainless steel or Inconel) and non-metallic (e.g. glass, alumina, or quartz).

Metallic sheaths are the most robust and easy to manufacture, but are also the most likely to cause contamination. They are generally best suited to use below about 450 °C and preferably below 250 °C. At higher temperatures, the metal atoms in the sheath become mobile and can diffuse to the element and ultimately contaminate the platinum wire. For use at temperatures above 250 °C, stainless steel and Inconel sheaths should be heat-treated in air or oxygen before assembly, to oxidise the inside surface of the sheath and to drive off lubricants used in the drawing process. Glass elements and glass-encapsulated ceramic elements, which are less susceptible to contamination by the sheath, may be more suited to use above 250 °C.

At temperatures above 450 °C all platinum elements become very susceptible to contamination, and any metallic part of an assembly is a potential source of impurities. It is therefore essential to maintain the highest levels of purity for all components. Above 600 °C some metals can migrate through quartz, and quartz sheaths also suffer from devitrification whereby impurities cause it to transition from a glassy to a crystalline structure, which is more porous and very brittle.

The length of the sheath should be chosen according to the application and temperature range. As a guide, the minimum sheath length should be about 200 mm plus 100 mm per hundred degrees of duty above 200 °C. For example, a minimum length for use at 400 °C is 400 mm.

3. Instrumentation

The preceding discussion of resistance thermometry pre-supposes the ability to make the necessary electrical measurements. The resistance measurement of IPRTs poses three key problems that will have an impact to a lesser or greater extent in different applications. These are described in turn.

3.1. Probe and connections

3.1.1. *Lead resistance*

Depending on the resistance measurement technique chosen, the resistance of the lead wires can influence the accuracy of the resistance measurement. The different methods are discussed in Section 4.4 below. For accuracies better than about 0.2 °C, 4-wire measurements should be made. This will have an impact on the cost of the IPRT assembly, including leads, and the cost of indicators and controllers.

3.1.2. *Thermal emfs*

Stray thermoelectric voltages (thermal emfs) are caused by temperature gradients in the measurement circuit. They can amount to several microvolts, and limit the accuracy of DC instruments to about 0.02 °C. The effects and solutions are discussed in detail in Section 4.6 below. For accuracies better than 0.02 °C it is necessary to use an AC measurement technique, such as an AC bridge or a bipolar DC bridge which actually uses a low-frequency square-wave sensing current.

3.1.3. *Self-heating*

The need to pass a current through the IPRT sensor to measure resistance means that heat is dissipated there, and the sensor is at a higher temperature than its surroundings. In applications measuring fluid temperatures (e.g. during calibration), this ‘self-heating’ effect is typically in the range 2 mK to 20 mK for 100 Ω sensors (for currents up to 1 mA). However, in applications where the IPRT is used in air, the self-heating may be as much as a few tenths of a degree. A detailed explanation of the effect is given in Section 4.1 below.

3.2. Verification and calibration of resistance bridges

Regular ice-point or triple-point measurements of IPRTs are needed to confirm the stability of the IPRT, but it is also useful to make periodic checks on the resistance bridge. There are two simple techniques for doing this, which do not require calibrated resistors.

3.2.1. *Zero and complement checks*

Consider a 7-digit AC bridge that measures the ratio of two resistances connected in series in a four-lead configuration (i.e. with two current leads and two voltage leads for each resistor, to sense the potentials generated). The first test is to check

that it correctly reads zero resistance. Most bridges have an option to check this, but otherwise a true zero resistance can be simply presented to it by connecting the two current input terminals together and the two voltage input terminals together, and linking them two by a short length of copper wire.

The bridge may also have an option for a ‘complement’ check, but if not it can be set to measure the ratio of two stable and nominally equal 100 Ω resistors. Two measurements are made: first the ratio R_1/R_2 which (for example) is 0.999987; and second, the resistors are swapped and a measurement of R_2/R_1 is made, which turns out to be 1.000015. Ideally, the product of the two measurements should be equal to 1.0; here it is 1.000002. The error in the product of the two readings is 2 counts in the last digit, indicating that the error in each of the individual readings is probably one count in the last digit. Note that it is possible that the bridge transformers have large errors that almost cancel, so the check builds confidence in bridge accuracy at ratio 1, but cannot prove that it is linear, i.e. that intermediate ratios are accurate. To do this requires other known resistance ratios to be generated, which can be done using standard resistors of suitable values. An alternative elegant solution to the problem is to use a ‘bridge calibrator’.

3.2.2. The linearity check

Consider a set of four resistors connected together so that they can be measured both individually, and in series, while retaining their four-lead electrical definition (Figure 3.2.1). Such networks, which are available commercially, are called Hamon resistors [Hamon 1954]. The network makes it possible to measure the linearity of a resistance bridge, as summarised in Table 3.2.1.

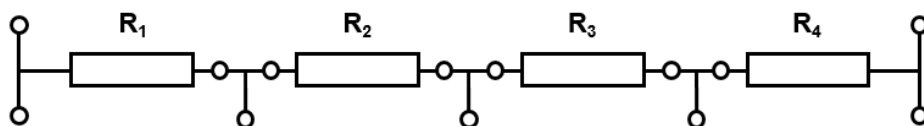


Figure 3.2.1. A simple resistance network that can be used to check the linearity of a resistance bridge. Note that each resistor can be measured as a four-lead resistor.

Table 3.2.1. Illustration of information used to inform the linearity check.

| Resistor | Measurements of individual resistors | Accumulated sum of individual measurements | Measurements of resistors connected together | Differences between measured and calculated sums |
|----------|--------------------------------------|--|--|--|
| 1 | 0.250 007 | 0.250 007 | 0.250 007 | 0 (by definition) |
| 2 | 0.250 015 | 0.500 022 | 0.500 020 | 0.000 002 |
| 3 | 0.250 002 | 0.750 024 | 0.750 026 | -0.000 002 |
| 4 | 0.249 994 | 1.000 018 | 1.000 019 | -0.000 001 |

The results in this example show that the bridge non-linearity is probably less than one or two counts in the last digit of the bridge reading. Note that the linearity check

is insensitive to errors proportional to readings, so as with the complement check, the linearity check is not a proof of absolute accuracy. However, if a ratio bridge is linear and the complement check is successful, it is also accurate. R_t and R_s are both multiplied by the same factor $(1 + \delta)$ and δ is small; in this case, the absolute accuracy (of resistance) comes only from the standard resistor. Systems for bridge calibration based on this principle (the ‘Resistance Bridge Calibrator’ [White 1997, White 2008, White 2013] are commercially available and can provide up to 70 individual points across the range of the bridge to quantify the linearity [Pearce 2016].

The availability of calibrations for resistance meters and bridges depends on the type and accuracy. Calibrations for DC and low frequency (< 0.1 Hz) switched DC meters are readily available from many national metrology institutes and the larger accredited electrical calibration laboratories. AC bridges can also be calibrated though the procedure may be more involved since these are typically for high accuracy applications, and very dependent on the measurement topology as well as the operating frequency, the current waveform, and other defining conditions.

3.3. Use of DC meters and industrial transmitters

The temperature instrumentation systems found in modern industrial environments are highly automated and tied into local area networks to provide continuous remote monitoring and maintenance functions [Liptak 2003]. The engineer or technician will often rely on software to perform some routine calibration and verification functions over those networked instruments. Once off-line, however, some simple bench tests may be useful to verify that a temperature readout is working properly. In many cases the verification of simple DC unipolar instruments and industrial transmitters requires only two spot checks near the upper and lower limits of the instrument range. This can be accomplished with the use of any of various resistance simulator instruments, or two calibrated resistors of the appropriate values. Values of $20\ \Omega$ and $300\ \Omega$ will be sufficient to cover a range from $-196\ ^\circ\text{C}$ to $558\ ^\circ\text{C}$ assuming a standard Pt100 input. Other spot check methods involve checking the IMP reading, $R(0\ ^\circ\text{C})$, on a recently calibrated IPRT and comparing that result against the reported value from a certificate or against the reading on another meter or transmitter that has been recently calibrated. Both handheld and benchtop (laboratory grade) temperature calibrators are commercially available to support the routine calibration requirements for these instruments. Calibration uncertainties in the range of 0.1 % to 0.02 % are readily achievable.

4. Limitations in performance

IPRTs are generally produced to match the (inter-) national standard specifications but the production is not 100 % reliable, since their performance is limited by several effects, such as self-heating, immersion, response time, lead resistance, insulation resistance, thermoelectric, electrolytic, and other DC effects, hysteresis and short term stability, and reproducibility and long-term stability. Tests for these effects are therefore necessary to select thermometers that match within closer tolerances.

4.1. Self-heating

Measurement of the resistance necessitates passing current through the thermometer. The resulting heating in the resistance element raises its temperature above that of the surroundings until the heat can be dissipated. There are two components in the self-heating effect: firstly, the internal heating effect, which leads to a difference in temperature between the platinum sensor and the protecting sheath, and is therefore a function of the thermometer design and construction; and secondly, there is an external heating effect which depends on the effectiveness of the thermal contact between the sheath and its surroundings, and is therefore dependent on the application. In well-designed situations, the external effect can be made small and the internal self-heating is dominant.

The self-heating is proportional to the power dissipated and hence to the square of the measuring current, i . Commonly, the IPRT resistance is measured at 1 mA and $\sqrt{2}$ mA, which dissipate a power of 100 μ W and 200 μ W in a 100 Ω PRT at 0 $^{\circ}$ C. The change in resistance can be plotted as a function of i^2 , see Figure 4.1.1, and extrapolated linearly to zero power (0 mA). If desired a correction may be made for the self-heating: in this example the power was doubled, so the change in resistance, $\Delta R = R(\sqrt{2} \text{ mA}) - R(1 \text{ mA})$, is equal to the self-heating at 1 mA, and resistance at 0 mA is $R(1 \text{ mA}) - \Delta R$. Clearly in making these measurements the external temperature should be kept constant, and time allowed for the readings to become steady. If the temperature is drifting, several cycles of readings at 1 mA and $\sqrt{2}$ mA may be needed to determine the difference reliably.

The linearity of the extrapolation of R as a function of i , namely

$$R(i) = \frac{R(i_2 \text{ mA}) - R(i_1 \text{ mA})}{(i_2^2 - i_1^2)} i^2 + R(0 \text{ mA}) \quad (4.1.1)$$

has been confirmed for many sensors, temperatures, and measurement currents (e.g. [Batagelj 2003]) at the microkelvin level. The uncertainty of the extrapolated value depends on the ratio of the currents used. This has been investigated [Pearce 2013, Veltcheva 2013] and an optimal value of (i_1/i_2) of about 0.56 was found if the measuring time is the same at both currents. The very lowest uncertainty can be achieved if the ratio is 0.5, and the measurement time at the lower current is 8 times longer to account for the poorer signal to noise ratio, which the analysis assumes is

inversely proportional to current. However, using currents in the ratio $1/\sqrt{2}$ is convenient and good enough for most purposes.

Many instruments for the measurement of IPRTs use a single measuring current, and thus cannot perform the measurement of the self-heating effect. In the calibration, the IPRT resistance measurements are usually performed with the same measuring current, typically 0.5 or 1 mA, and the results in the certificate are then given for this current. The subsequent use of the calibrated thermometer requires the resistance to be measured using an instrument working at the same measuring current as was used during calibration. However, if the medium is very different, e.g. in air rather than in a liquid, the self-heating effect will be significantly higher than that during calibration (see Figure 4.1.1). The self-heating error should then be evaluated by measuring the thermometer resistance *in situ* with an instrument using two currents, while the temperature is kept constant.

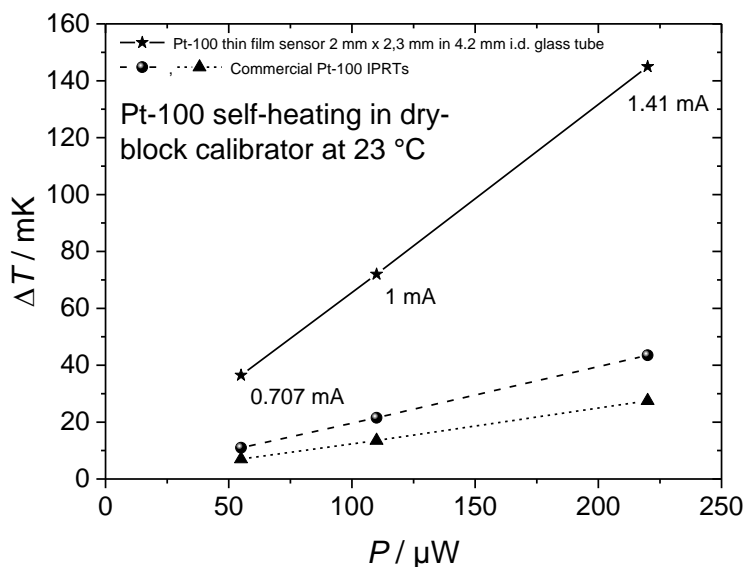


Figure 4.1.1. Self-heating effect as a function of applied power (i.e. as a function of measuring current squared), for two commercial IPRTs and a thin-film PRT in a glass tube, illustrating the effect of the thermometer construction on the magnitude of the self-heating effect [Rudtsch 2020].

Manufacturers usually specify the self-heating coefficient of their sensors, or IPRT probes, measured in a specific medium. Sometimes the coefficient is evaluated between 0 °C and 30 °C in flowing water with a velocity of about 0.4 m s⁻¹, or in flowing air with a velocity of about 3 m s⁻¹, and in other cases at 0 °C in a well stirred mixture of ice and water. The coefficient may be given in two forms:

- Self-heating coefficient, in units of °C/mW
- Dissipation constant, in units of mW/°C

The values for the self-heating coefficient of a IPRT range from 0.003 °C/mW for a bare sensor to 0.25 °C/mW for a probe (300 mW/°C to 4 mW/°C).

A common assumption made by users is that performing measurements in terms of the ratio to the resistance at the ice point ($R(t) / R(0\text{ }^\circ\text{C})$) provides some level of cancellation of the self-heating error around the temperature of use; if the thermal resistance between the sensor and environment is constant, the self-heating would scale with the resistance, and the cancellation would work over a wide temperature range. However, it has been demonstrated that is not always the case [Ballico 2014]; measurements of 6 SPRTs and 6 IPRTs, of different designs, showed that PRT self-heating varies from being almost constant with temperature to being nearly proportional to temperature (or sensor resistance and dissipation).

4.2. Immersion

In an ideal temperature measurement, the sensing element of the thermometer is at the same temperature as the medium in which it is immersed. Unfortunately, the lead-wires and sheath of the typical IPRT assembly provide a thermal path for heat transfer between the medium and the ambient environment. The conduction of heat along the thermometer causes a small error which decreases as the immersion of the thermometer increases. Theoretical models of the immersion error have been developed for thermometers [Kerlin 1982, Nicholas 2001] and for IPRTs in industrial thermometer wells [Benedict 1963]. Examples of the application of this type of model are given in [White 2010b].

A simple first-order model of immersion effects suggests a temperature error given by:

$$\Delta T_{\text{imm}} = T_{\text{meas}} - T_{\text{sys}} = (T_{\text{amb}} - T_{\text{sys}}) K e^{-L/D_{\text{eff}}} \quad (4.2.1)$$

Where T_{amb} is the ambient temperature near the protruding sheath of the thermometer, T_{sys} is the temperature of the medium being measured, K is a constant depending on the thermal properties of the thermometer and the medium, L is the length of thermometer immersed in the medium, and D_{eff} is a constant related to the diameter of the thermometer and certain heat transfer properties of the sheath and related construction materials (and generally needs to be parameterised to experimental data).

The immersion error can be estimated by measuring the observed temperature as a function of the immersion depth and plotting the relative error, $(T_{\text{sys}} - T_{\text{meas}}) / (T_{\text{sys}} - T_{\text{amb}})$ versus the immersion depth. Figure 4.2.1 shows the immersion profile of two IPRTs in a stirred-oil bath. The data for the 10 mm diameter IPRT are very consistent with the model equation, except that the slope on the line corresponds to an effective diameter, D_{eff} of about 26 mm. The data for the 4 mm IPRT additionally show the effect of the finite length of the sensing element in the first 30 mm of the immersion curve. Once the sensing element is sufficiently immersed the curve again follows the simple first-order model.

Where possible the IPRT should be immersed sufficiently to ensure that the immersion error is negligible for the required purpose. Small sensor size, small

diameter sheaths, directly immersed in low viscosity fluids have a distinct advantage.

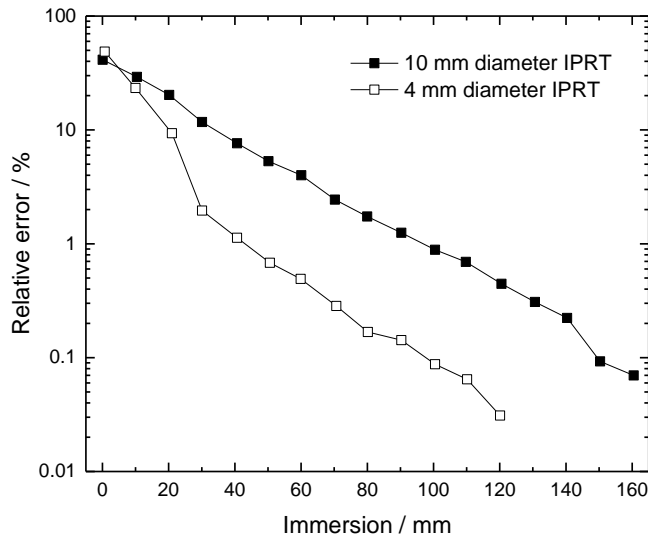


Figure 4.2.1. Example immersion characteristics of two IPRTs with different diameters.

A more sophisticated model of the immersion error was developed by White and Jongenelen [White 2010b] and compared with extensive immersion profile measurements for IPRTs under a range of different conditions. The results are expressed in terms of temperature error as a function of immersion, where the immersion depths are expressed as multiples of the IPRT sheath diameter. This is shown in Figure 4.2.2.

In general, the first 10 diameters of immersion ensure the relative temperature error is $< 1\%$, and each additional 10 diameters of immersion further reduce the error by at least a factor of 10.

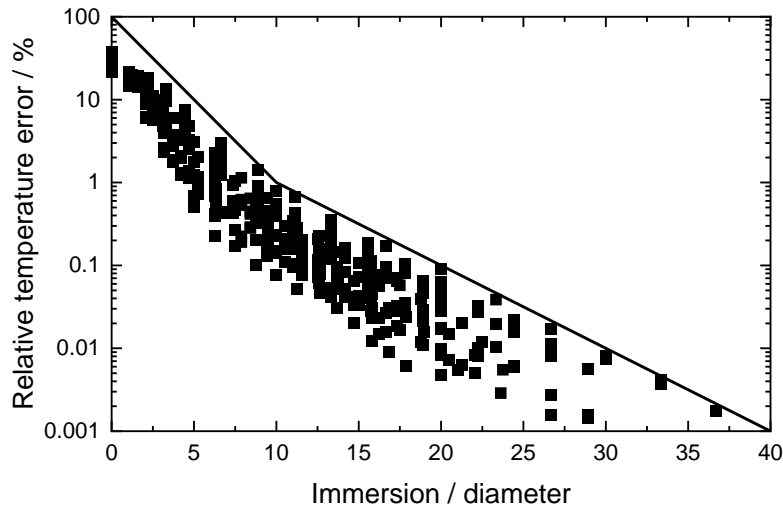


Figure 4.2.2. All immersion data for IPRTs in oil baths, with the immersion expressed as multiples of the IPRT diameter. The line gives an approximate upper bound to the relative temperature error [White 2010b].

Another important error related to immersion is due to radiative heat transfer. The radiative error for an air temperature sensor in flowing air depends on the sensor diameter and the air speed, with smaller sensors and higher air speeds yielding values closer to true air temperature [de Podesta 2018]. Harrison [Harrison 2015] clearly explains the basic physics of the interaction of a temperature sensor with flowing air and arrives at the prediction that the radiative error of a thermometer depends on the square root of the diameter of the sensor and inversely on the square root of the air speed past the sensor. This is exemplified by an influential study which shows that in sunshine, thermocouple sensors with different diameters (up to about 0.5 mm) exposed to wind speeds between 0.2 m s^{-1} and 1.2 m s^{-1} exhibit errors of up to $4 \text{ }^{\circ}\text{C}$ [Bugbee 1996], with the error increasing as the sensor diameter increases, and as the air speed decreases. This is due to the radiative heating of the thermometer by the sun; the principal influence of the sensor diameter is due to the balance of heat transfer between the radiative heating and the heat transfer with the surrounding air; as the sensor diameter decreases, the balance of heat transfer shifts in favour of the surrounding airflow and the error due to radiative heating decreases.

4.3. Response time

Just as with self-heating, the response time of a thermometer depends on both the characteristics of the thermometer and of the medium in which it is immersed. A simple first order model based on the thermal mass and thermal conductivity of the thermometer suggests a simple exponential response giving rise to a time dependent error, following a step change from its initial temperature, T_{init} , into a system at a temperature T_{sys} , of:

$$\Delta T = (T_{\text{init}} - T_{\text{sys}})e^{-t/\tau} \quad (4.3.1)$$

Where t is the time in seconds, and τ is the time constant of the thermometer. While (4.3.1) is a good first approximation for thermometers that are thermally homogeneous, thermometers comprising sheaths, thermowells, internal insulating materials, etc. in addition to the sensing element, exhibit more complex responses. Kerlin et al. [Kerlin 1982] also highlight the importance of the thermal conductivity and thickness of the boundary layer of the fluid surrounding the thermometer, and the diameter of the thermometer: time constants generally increase with the square of the diameter.

Thus, the thermal response of the thermometer to a step change can be more generally modelled as a series of terms [Kerlin 1982]:

$$T(t) = A_0 + A_1e^{-t/\tau_1} + A_2e^{-t/\tau_2} \quad (4.3.2)$$

where A_0 , A_1 , A_2 , etc., are temperature pre-multipliers, τ_1 , τ_2 , etc., are the time constants for the various barriers to the flow of heat between the resistor and the external system. There are two methods to determine the response. The first consists of plunging the thermometer into a fluid, measuring the response under these conditions, and then deducing the response times in the medium to be used using the model equation. The second method consists of studying, in situ, the response of the thermometer by using the thermometer resistance itself as a heating element. Then, by analysing the response when the thermometer ‘heater’ current is reduced to its measurement value, one can obtain the response time using an algorithm (e.g. [Kerlin 1982]). The two methods yield different responses, but have similar model time constants. Figure 4.3.1 illustrates the response time measured with a 10 mm diameter sheathed IPRT.

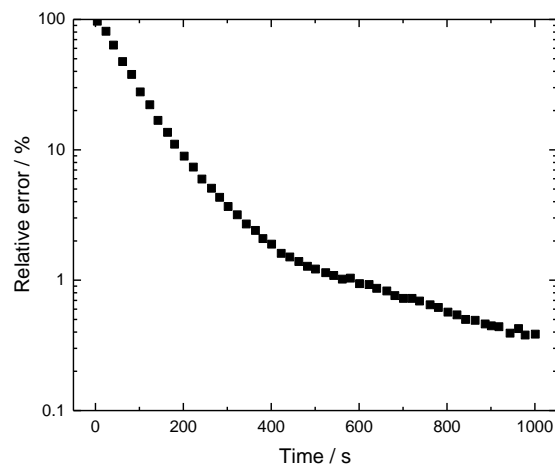


Figure 4.3.1. The measured response of a 10 mm diameter sheathed IPRT immersed in a stirred oil bath. The two different slopes on the line and the slight downward curvature in the first few seconds indicate a system with three distinct time constants.

An example of the first method was the measurement of the response time of Pt100 film resistance temperature sensors by switching two air fluxes flowing on the tested thermometer, one at 25 °C and the other at 50 °C [Cimerman 1999]. Under certain conditions the probe error can be approximated by an equation of the form:

$$\Delta T = A_1 \frac{\tau_1}{\tau_2 - \tau_1} e^{-t/\tau_1} - A_2 \frac{\tau_2}{\tau_2 - \tau_1} e^{-t/\tau_2} \quad (4.3.3)$$

where t is elapsed time. τ_1 characterises the initial response and τ_2 characterises the longer-term behaviour of the thermometer. For the thermometers tested, τ_1 values ranged from 1.5 s to 9.4 s depending on the assembly and the position in the probe sheath, and in all cases τ_2 was found to be between 34 s and 40 s.

4.4. Lead resistance

In principle, a single voltage measurement and a single current measurement are sufficient to determine the resistance of a sensor. In resistance bridges, the two are combined by measuring the ratio of the voltages across the sensor resistor, $R(t)$, in series with a known resistor, R_s , when the same current is flowing in both, in which case $R(t) = (V(t)/V_s)R_s$.

In practice, there are many small effects that introduce errors into the measurements.

Most resistance measurements are performed by connecting the resistance measurement instrumentation to the sensing element with 2, 3 or 4 wires. With 2-wire measurements the error is largest because the leads resistances are included in the measurement. With 3-wire systems (there are several types) some compensation for leads resistances is achieved, but residual errors remain. In principle, for 4-wire systems the resistance of the leads can be eliminated, but the situation is more complicated than that because the sensitivity to lead resistance depends on the impedance of the current source of the voltmeter which should, ideally, be infinite.

Many different methods have been developed to reduce the effects of the errors due to leads resistances. The following is applicable to both DC and AC measurements, although in some cases there may be some subtleties associated with DC measurement; for more details see [White 2017].

4.4.1. Two-wire resistance measurement

In a two-wire resistance measurement, Figure 4.4.1, the lead resistances are indistinguishable from the resistance of the sensing element, and the measured resistance is:

$$R_{\text{meas}} = R(t) + R_{L1} + R_{L2} \quad (4.4.1.1)$$

where $R(t)$ is the resistance of the PRT and R_{L1} and R_{L2} are the resistances of the two leads. The inclusion of the lead resistances in the resistance measurement causes an error in the temperature measurement of approximately:

$$\Delta T = 2R_L \left(\frac{dR}{dT} \right)^{-1} = \frac{R_{L1} + R_{L2}}{R_0 \alpha} \quad (4.4.1.2)$$

where α is the relative temperature coefficient of the IPRT, typically $0.00385 \text{ }^\circ\text{C}^{-1}$, and R_0 is the nominal resistance of the IPRT. For a sensor with $R_0 = 100 \text{ } \Omega$ the error is typically of the order of $2.5 \text{ }^\circ\text{C}$ per Ω of total lead resistance. Since the lead wires may have as much as $0.1 \text{ } \Omega$ resistance per metre, the error could be significant in some installations.

Many direct reading instruments (i.e., reading in $^\circ\text{C}$) that employ the two-wire resistance measurement method have an offset adjustment to compensate for this error, at least over a modest temperature range. However, R_L is temperature-dependent, and any change to the leads, such as the use of extension leads or long-term damage to the leads or connectors, will also change the error. Note that the error decreases as R_0 increases. The reduction in lead-resistance error is one of the main benefits of high resistance ($1000 \text{ } \Omega$ or $2000 \text{ } \Omega$) thin film IPRTs. With the $100 \text{ } \Omega$ sensors, the best accuracy achievable for two-wire measurements, with adjustment, is about $0.2 \text{ }^\circ\text{C}$.

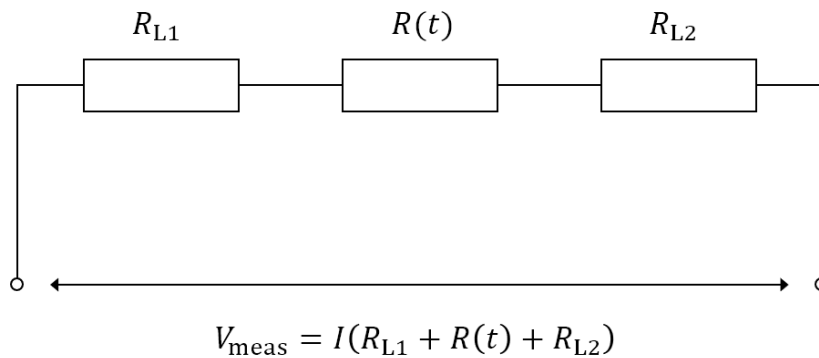


Figure 4.4.1. A 2-wire resistance measurement showing the lead resistances (after [White 2017]).

4.4.2. Three-wire resistance measurement

A more effective method of compensating for lead resistance is to include a third lead to the IPRT, and three-wire measurements, Figure 4.4.2, are commonly employed in industrial situations. The method enables two lead resistances R_{L1} and R_{L2} to be connected in opposing sides of the bridge network, so their effects are partially compensated in the bridge balance, and the third lead is connected to the bridge output amplifier. With this circuit the voltage across one side of the bridge, $I(R(t) + R_{L1})$, is compared with the opposing voltage $I(R_2 + R_{L2})$, where the resistor R_2 is matched to $R(t)$ at some point. The voltage ratio approximates to

$$(R(t)/R_2) * (1 + (R_{L1}/R(t) - (R_{L2}/R_2))) \quad (4.4.2.1)$$

Hence if R_{L1} and R_{L2} are equal, full compensation is achieved when $R(t) = R_2$, but it gradually becomes poorer as the temperature increases or decreases from this point.

Alternatively, if the voltage drop across one of the lead resistances is also measured (R_{L2} in Figure 4.4.2), it can be subtracted from the primary measurement. The resulting measured resistance for the 3-wire method is then:

$$R_{\text{meas}} = R(t) + R_{L1} - R_{L2} \quad (4.4.2.2)$$

and the error in the temperature measurement is:

$$\Delta T \approx \frac{R_{L1} - R_{L2}}{\alpha R_0} \quad (4.4.2.3)$$

This three-wire system therefore eliminates the need to compensate for the lead resistance, but it still requires the three lead resistances to be equal.

Three wire circuits find wide use in industrial plants where cable lengths can be long (though in that case a 4-20 mA transmitter might be preferred). The potential accuracy of three-wire circuits is variable, but substantially better than the adjusted two-wire systems, < 0.1 °C.

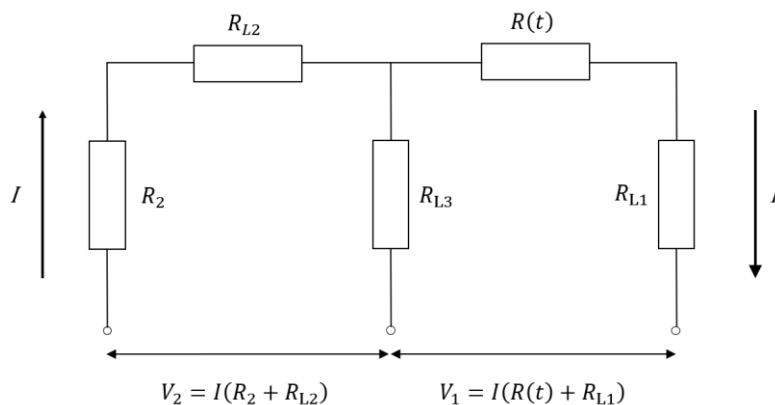


Figure 4.4.2. The 3-wire resistance measurement in a Wheatstone bridge, in which the voltage in the right-hand side, $I(R(t) + R_{L1})$, is compared with the voltage in the left, $I(R_2 + R_{L2})$. R_{L3} is connected to one side of the output amplifier, and the two other fixed bridge resistors R_3 and R_4 in the circuit are not shown.

4.4.3. Four-wire resistance measurement

Ideally the resistance of the IPRT should be measured using the 4-wire method, which separates the current and voltage measurements. In this method, Figure 4.4.3, the sensing current is passed through one pair of leads and the voltage is measured using the other pair of leads. Because there is no current flowing through the voltage leads, there is no voltage drop in those leads and there is no lead resistance error. The circuit current is measured by comparing the voltage across $R(t)$ with that across a known resistor R_s , in series with it, from which $R(t) = (V(t)/V_s)R_s$.

Most IPRT sensing elements are supplied as two-wire devices, so manufacturers of finished IPRTs weld a pair of lead wires to each of the element leads to make four-wire connections at some point near the ceramic body of the element, but external to the ceramic itself. This means that a small portion of the external lead wires (typically 6 mm to 10 mm of a Pt-Rh alloy wire, ~ 0.2 mm diameter) will in effect be included in the measured resistance. This may add ~ 1 mΩ of external lead resistance to the total measured resistance, or about 0.001 % for a Pt100. This has no practical effect on the performance of most IPRTs, except in the case where there is no sheath to immobilise the leads and these small portions of lead wire are exposed to external forces. In that case external stress on the lead wires can be transmitted to the other portions of the platinum sensing element and small strain-induced resistance changes can occur.

The lead-resistance effects in good four-wire measurements are practically zero (but see the introduction to this section). Instruments employing the four-wire measurements are preferred for laboratory applications and for reference thermometers. AC and DC measurements can achieve accuracies of better than 0.001 °C.

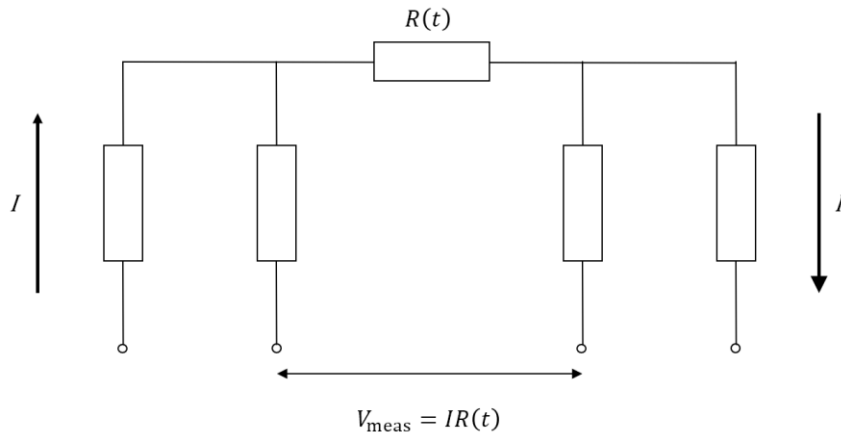


Figure 4.4.3. A 4-wire resistance measurement (after [White 2017]).

4.5. Insulation resistance

Accurate resistance measurement requires all the sensing current to pass through the resistance. The effects of any leakage resistance or poor electrical insulation are well modelled by the insulation resistance R_{ins} connected electrically in parallel with the sensing resistance $R(t)$:

$$R_{\text{meas}}(t) = \frac{R(t)R_{\text{ins}}}{R(t)+R_{\text{ins}}} \approx R(t) \left(1 - \left(\frac{R(t)}{R_{\text{ins}}} \right) \right) \quad (4.5.1)$$

Therefore, the effect of poor insulation is to decrease the measured resistance, and the effect increases with the ratio of $R(t) / R_{\text{ins}}$. Leakage resistance or insulation effects have several known causes.

At high temperatures all insulating materials break down and conduct to some degree. Given sufficient thermal energy, electrons are excited into conducting states, so that the insulator exhibits the resistance-temperature characteristic of a semiconductor:

$$R_{\text{ins}}(T) = R_0 e^{E_g/2kT} \quad (4.5.2)$$

Where E_g is the band-gap (excitation) energy and T is the temperature in kelvin. The insulation resistance therefore falls exponentially with increasing temperature. The best insulation materials are those with large band-gap energies, including fused silica and alumina. Impurities in the materials provide intermediate electronic states, effectively lowering the band-gap energies and significantly lowering the insulation resistance. For the same reasons, glasses, which are amorphous mixtures of oxides, are of limited use at high temperatures. For high accuracy applications very high purity insulation materials should be used. The use of high purity substrates is a feature of IPRTs made for temperatures above 600 °C.

One particularly common insulating material for IPRTs is magnesia (magnesium oxide, MgO). Unfortunately, magnesia has an affinity for water, so IPRT assemblies using magnesia must be hermetically sealed to prevent the ingress of moisture and the development of leakage resistance problems. The moisture becomes apparent as a hysteresis effect (Section 4.7) and can be detected by using a low voltage (< 100 V) insulation tester to measure the resistance between the lead wires and the external steel sheath. Ideally the insulation resistance should exceed 100 MΩ, but moisture can cause it to be as low as a few kilo ohms. In poorly manufactured probes the moisture may be sealed in at the time of manufacture. IPRTs with long sheaths or those operated in wet or humid environments are particularly prone to developing the effect over months or years. Where long cable lengths are used, the insulation surrounding the lead wires becomes important. Most commonly, problems occur with long lengths of PVC insulated cable: highly pigmented (coloured) or old PVC is particularly prone to poor insulation resistance. Most IPRT manufacturers can supply cables with PTFE (Teflon®) insulation, which has far superior insulation properties.

Glass encapsulated platinum sensors can exhibit a rather insidious leakage effect if used with AC resistance bridges and at high temperatures. At temperatures within about 150 °C of the softening point of glass, the glass begins to behave as a lossy capacitor, so effectively shunting the sensing resistance. Glass encapsulated IPRTs should not be used in conjunction with AC bridges in applications above 200 °C.

4.6. Thermoelectric effects, DC and AC measurements

4.6.1. DC measurements

Most instruments used to measure the IPRT resistance use a DC sensing current and voltage measurement. Therefore, any extraneous voltage induced in the measurement circuit will induce an error. The equivalent temperature error caused by the stray voltage V_{stray} is:

$$\Delta T_{V_{\text{stray}}} = \frac{V_{\text{stray}}}{I_0 R_0 \alpha} \quad (4.6.1)$$

where I_0 is the sensing current, R_0 is the ice-point resistance of the IPRT and α ($\sim 3.85 \cdot 10^{-3} \text{ }^\circ\text{C}^{-1}$) approximates the temperature coefficient of the IPRT. V_{stray} may be about 1 μV , and for a 100 Ω sensor, the error is then about 2.5 mK.

There are several potential sources of stray emf in most resistance measurements including thermoelectric effects, and the offset voltages of amplifiers. It is also possible that stray current from input bias currents of amplifiers, electrolytic effects (due to the presence of moisture and different metals) and ground loops can induce stray voltages. For most of these effects, careful circuit layout, the use of grounded metal-sheathed probes, and good hermetic seals on IPRT assemblies will eliminate the effects. However, the thermoelectric effects are difficult to avoid.

Thermoelectric voltages are induced by temperature gradients on the lead wires. Normally the voltage on one of the leads is balanced by an equal voltage on the other lead. However, if a mix of different metals (e.g., copper and platinum) is used for the leads, or there are temperature gradients where the connections are made, then it is possible that the thermoelectric voltages do not balance each other. Even damage to copper leads can lead to small stray thermoelectric effects. Typically, the effect is at the level of several microvolts so the temperature errors may be of the order of 0.01 $^\circ\text{C}$. This has practically no effect on most industrial applications but may be the limiting factor in the performance of many commercial electronic thermometers such as those used as mid-accuracy reference thermometers and in testing laboratories.

One simple way of eliminating thermoelectric effects is to make two measurements of resistance, one with the current reversed in relation to the other, and to average the two results. If the thermal emfs are constant they have no effect on the average and are eliminated from the measurement. This is the principle underlying all so-called DC bridges: they are in fact AC bridges using a very low frequency (0.01 Hz to 5 Hz) square-wave sensing current. Many of these bridges achieve accuracies in resistance measurements approaching 1 m Ω so the resulting uncertainties are negligible by comparison with other effects on the temperature measurement. The best can deliver uncertainties rivalling those of AC bridges; see below.

An alternative method of eliminating thermal emfs, used by many digital multi-meters and some electronic resistance thermometers, is to measure the stray voltage when the sensing current is zero and use this measurement to offset the voltage error in the resistance measurement. Commercial instruments are available that

measure with accuracies of about 200 m Ω (less than 1 mK equivalent for 100 Ω sensor).

4.6.2. AC measurements

Thermoelectric and other DC effects are in principle avoided by making true AC measurements. These use a sinusoidal sensing current, typically in the frequency range 10 Hz to 400 Hz. Instruments of this type are based on the accurate balance between the AC voltage across the resistance thermometer and that obtained from a voltage ratio divider (transformer) connected to a reference resistor. The accuracy of an AC bridge depends essentially on the linearity of its voltage ratio divider, but most bridges reach accuracies at the level of 0.001 °C or better. It is fundamental for accurate measurements with an AC bridge to completely annul the ‘quadrature’ component in the measuring voltage, which arises principally from stray inductances and capacitances in the lead wires to the sensor. In many industrial applications, where long leads are required to the IPRT assemblies, instruments based on AC bridges may not be able to automatically compensate for the additional capacitive and inductive components of the leads.

AC bridges are generally preferred for IPRTs at high temperature, where large temperature gradients could induce significant and unstable stray thermal emfs in the measuring circuit.

4.7. Hysteresis and short-term stability

IPRTs exhibit hysteresis on thermal cycling; this means that the IPRT may have different but reproducible R versus T relationships depending on the thermal history of the thermometer and on whether a given temperature is being approached from lower or higher temperatures [Curtis 1982]. Hysteresis is a key performance parameter for IPRTs used in high-accuracy applications. A classic example of hysteresis is shown in Figure 4.7.1. In IPRTs there are three main causes of hysteresis: mechanical strain, moisture, and oxidation.

4.7.1. Mechanical

Mechanical hysteresis arises from the difference in thermal expansion between the platinum wire and the ceramic or glass substrate on which the platinum wire is mounted. As the temperature changes, the differential expansion causes the wire to become compressed or stretched, leading to the distortion of the wire and an effect on its resistance. Strain gauges work using the same principle. In IPRTs, if the strain is sufficiently large then the wire will slip against the substrate and relax. When the temperature change is reversed the compression/stretching effect is opposite and the sensor shows a resistance error in the opposite direction. Thus, the resistance/temperature relationship for the sensor is different depending on whether the temperature is increasing or decreasing.

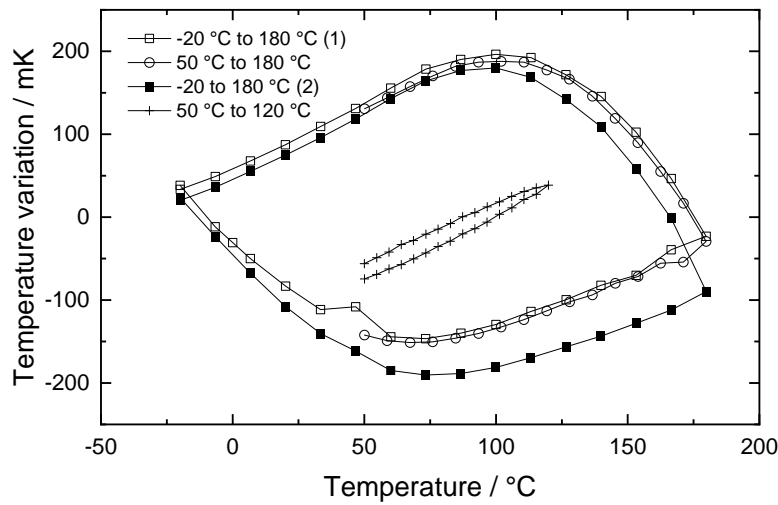


Figure 4.7.1. An example illustrating the potentially large mechanical hysteresis effect in an IPRT [White 2010].

In all IPRTs a compromise must be made between the ability of the thermometer to withstand shock, vibration, and mechanical hysteresis. In fully supported IPRTs the wire can become stressed and work-hardened if it is exposed to vibration or shock. Such sensors are particularly useful, for example, in aircraft, but because of the intimate contact with the substrate it is particularly susceptible to hysteresis. Figure 4.7.1 is near the extreme of hysteresis observed in practice: about 0.1 % of the temperature range. Similar effects have been observed by [Besley 1983, Chattle 1975, Chattle 1977] on cycling between -200 °C and 100 °C . Thin-film IPRTs also exhibit hysteresis of comparable magnitude and stability between 0 °C and 500 °C [Gam 2011, Zvizdic 2013]; additionally, Zvizdić [Zvizdic 2013] showed that the magnitude of the hysteresis for thin-film IPRTs also depends on the speed of the temperature change. Ljungblad [Ljungblad 2013] demonstrated that the hysteresis is typically a much more important effect than sensor stability, at least up to 500 °C .

Partially supported IPRT sensors typically have only part of the platinum wire bonded to the substrate. In coiled constructions for example (see Figure 2.3.1) it may be only one side of the coil that is bonded. This construction offers much reduced hysteresis and some immunity to vibration, but work hardening will still occur for high vibration and sharp mechanical shocks. There is a considerable range of construction methods for IPRTs, all offering slightly different compromises. For the best IPRTs, the hysteresis may be as low as 0.001% (1 mK hysteresis loop for 100 °C temperature range). In some constructions for applications near room temperature, the sensor may be oil filled to further damp vibrations while retaining low hysteresis.

A procedure should be followed to bring the IPRTs to an appropriate stable state suitable for accurate measurements. Since the hysteresis behaviour is caused by reversible changes in resistance from annealed to strained conditions in the platinum (at least below the temperature range where hysteresis due to reversible oxidation of the platinum can also occur), this means that the IPRT must be strained

for work below room temperature and annealed for work above room temperature and, subsequently, all thermal cycling must never exceed the limits of this stabilisation cycle. Consequently, since the thermometer is almost always stored at room temperature, the temperature should be maintained within the range of stabilisation, i.e., if stabilised below 100 K (strained), keep at room temperature or below; or if stabilised at 200 °C to 450 °C (annealed), keep at room temperature or above⁴.

For thin-film resistors especially the hysteresis may be reduced by repeated cycling; in one study, repeated cycling of 30 IPRTs between 0 °C and 500 °C reduced the magnitude of the hysteresis by a factor of 10, and it was found that in general the thermal hysteresis was in the range from 16 mK to 156 mK for all these sensors [Gam 2011].

It has been shown [Rusby 2017] that it is desirable to undertake preliminary cycling tests of IPRTs over the relevant temperature range, with ice-point checks after each temperature excursion, before beginning the calibration. This indicates the stability that may be expected and may condition the sensors to greater stability. It is also desirable to test for hysteresis by repeating measurements at the midpoint of the relevant temperature range, and it was suggested that ice-point measurements be repeated the day after a temperature excursion, before continuing the calibration, to establish whether relaxation of the sensing element has taken place overnight. With a selection of 'typical, good' IPRTs, hysteresis was < 0.0025 °C between 0 °C and 100 °C, and < 0.0035 °C when the range extended down to -80 °C or up to 150 °C. Greater instability occurred when sensors were cooled to -196 °C.

It has been shown that the amount of hysteresis is very dependent on the design of the sensing element and the temperature range, and that some sensors exhibit a large change in resistance on first use, whereas others show a slow increase in resistance with use. [White 2010] observed hysteresis ranging between 0.2 % of the temperature range for one glass-encapsulated sensor, see Figure 4.7.1, and 0.002 % for the best of the partially supported ceramic sensors studied.

4.7.2. *Moisture*

Hysteresis may also be caused by moisture inside the IPRT assembly. Water in the insulating material shunts the sensing current between the lead wires within the assembly, and within the sensor itself. The effect is particularly common in magnesia insulated constructions because of the affinity of the magnesia for water and the generally poor hermetic end seal on most IPRT assemblies. As the IPRT assembly is cycled in temperature the moisture migrates to different parts of the assembly causing different shunting effects and hence hysteresis. In [Mangum 1984] moisture was observed to produce changes as large as 35 mK on a sensor

⁴ There will be relaxation during storage. If a sensor is cycled below and above room temperature it will show hysteresis at room temperature, but if it is stored at room temperature it will tend to relax back to its 'natural' value. If it is then used above room temperature it will show a smaller hysteresis loop, and similarly if it is used below room temperature. The full hysteresis will once again apply if it is used over the complete range (but cycling rates will also affect the behaviour and relaxation may be slower or even non-existent at low temperatures).

cycling between 0 °C and 40 °C. Moisture (69 % of the cases) rather than strain (19 % of the cases) was believed to account for most of the drift in IPRTs seen in tests on 94 IPRTs in the range 0 °C to 100 °C (and with annealing up to 235 °C). Vented IPRTs should not be used below room temperature, to prevent moisture ingress, though it may be possible to dry them. A study of IPRT failures in power plant installations [Hashemian 1990] showed that about 16 % of IPRT failures were due to moisture intrusion into the sheath from leaks through defective or otherwise imperfect end seals.

The ASTM E644-11 standard [ASTM E644] contains a test method (Section 18) for End-Seal Integrity by monitoring the thermometer's insulation resistance under a thermally induced pressure differential. The pressure differential is transient, but sufficient to allow water vapour to be driven through any leaks which may exist in the end seal. The ingress of water through any leaks is revealed by an altered insulation resistance.

It has been shown that the presence of moisture in SPRTs can be detected by observing the difference between AC and DC resistance measurements [Marcarino 1999], and it is reasonable to expect this to apply to IPRTs too. This should be done at a temperature close to 0 °C where the effect is most pronounced.

The 'wetness parameter' for SPRTs may indicate the presence of water too [Strouse 2008]. There are three tests, which can also be used for IPRTs:

- Measure $R(\text{TPW})$ of the thermometer at a set of currents of I_1, I_2, I_1 , where the power dissipation at current I_2 is sufficient to raise the element temperature by > 1 mK or otherwise well above the noise limit of the measurement system. The two resistance readings at I_1 should repeat to within the noise limit. A lower second reading at I_1 (by more than 0.1 mK) may indicate that water within the sheath of the thermometer has condensed on the sensor and that the condensed volume is partially redistributed in response to local heating.
- The time required to reach equilibrium at the TPW from ambient conditions can indicate the presence of moisture. A 'dry' thermometer will effectively reach equilibrium (within a few tenths of a mK) within about five minutes; a 'wet' one will take longer.
- The sheath of the thermometer can be placed through the bottom of a polystyrene cup so that the rim of the cup is near the head of the thermometer. After allowing the thermometer to equilibrate at the TPW, the cup is filled with crushed dry ice. If the thermometer is 'wet', the condensed water will move from the sensor to the dry ice location along the thermometer sheath and a different $R(\text{TPW})$ will be measured.

4.7.3. Oxidation

Another cause of hysteresis is the oxidation effect that can, in certain circumstances, be observed in the behaviour of the IPRT sensors having the platinum wire in contact with air, such as for the coiled types shown in Figure 2.3.1. The oxidation effect was very well studied by Berry for the SPRTs [Berry 1982, Berry 1982b]. At temperatures between 450 °C and 560 °C, a film of orthorhombic

β -phase PtO₂ will form on the surface of platinum heated in air. It will dissociate rapidly in the temperature range 600 °C to 650 °C. This outer layer of oxide reduces the conducting cross-sectional area of the platinum and thus increases the resistance. Since the changes in resistance can be ascribed simply to dimensional changes, the PRT resistance ratio $R(t)/R(0\text{ °C})$ remains unchanged for a particular state of oxidation. Therefore, the hysteresis caused by the oxidation effect is evident only in the range between 450 °C and 650 °C. The consequent changes in resistance typically do not exceed 0.1 °C. There is also evidence that smaller changes in resistance occur as a result of oxidation that takes place in air at temperatures between 100 °C and 250 °C. These are probably due to a very thin two-dimensional oxide layer which forms in this temperature range, but which dissociates at about 300 °C. The consequent changes in resistance for this oxidation effect normally do not exceed a few millikelvin. Above 600 °C, however, severe oxidation effects can arise. A comprehensive discussion of oxidation effects on platinum is given in [Jursic 2014].

Impurities in the platinum may also be responsible for instabilities in IPRTs, if they influence the oxidation state of the host platinum, on the surface or internally. At high temperatures the impurities and their oxides may migrate and become locked at grain boundaries.

4.7.4. Characterisation of hysteresis

Although hysteresis is a key performance parameter for high accuracy applications, little has been published on the effect, and much of what is known is probably proprietary [White 2010]. Curtis [Curtis 1982] has proposed a test to quantify the magnitude of the effect for a given IPRT by cycling between –196 °C (liquid nitrogen) and 200 °C, and measuring the difference between the ice-point readings on the rising and falling temperatures. The observed differences provide indicative values for uncertainties to be included in the calibration uncertainty. Murdock and Strouse [Murdock 2009] performed this test for a large number of IPRTs, and observed key differences between sensor types, with the partially-supported sensor element types being the most stable.

Rusby and Machin [Rusby 2017] performed a study of hysteresis of a randomly selected cohort of (wire-wound) IPRTs and concluded that wire-wound IPRT sensors can be repeatable on cycling, at least up to 150 °C and down to –50 °C, with quite modest hysteresis, < 0.003 °C, less than has sometimes been reported. Further specific conclusions were that:

- It is desirable to undertake preliminary cycling tests of IPRT sensors over the relevant range, with ice-point checks after each temperature excursion, before embarking on the calibration. This should indicate the level of stability to expect and may condition the sensors to induce greater stability.
- As well as checking ice-point stability during the calibration, it is desirable to test for hysteresis by repeating measurements at the mid-point of a temperature excursion or the complete span. It is important that this is done before the sensor returns to ambient temperatures.

- Ideally ice-point measurements would be repeated the day after a temperature excursion, before continuing the calibration, to establish whether relaxation has taken place overnight.

4.7.5. *Specific hysteresis test procedures*

Recently three specific test procedures have been investigated:

- In the IEC 60751 standard [IEC 60751], section 6.5.6, it is recommended to measure the resistance in the middle of the temperature range after the thermometer is exposed to a temperature at the lower limit of the range, and then again at the same midpoint temperature after exposure to the upper limit temperature. The difference between measured resistances should not be larger than the tolerance value at the test temperature for the respective class.
- In Section 16 of the ASTM E644 standard [ASTM E644], another hysteresis test is described. This defines hysteresis testing as a means to quantify the amount of change in a IPRT when exposed to thermal cycling. The procedure is to start at ambient (room) temperature, then raise the temperature of the test thermometer to a specified maximum temperature (± 5 °C), then reduce the temperature to midway between the specified maximum and minimum temperatures and measure the reading. The temperature is then further reduced to the specified minimum (± 5 °C) and then raised to the midpoint temperature, when the second reading is taken. Several cycles should be performed in this way, and the average of measured resistance difference used to quantify the hysteresis.
- A third method commonly used by National Metrology Institutes is to use a similar procedure to those above, with the difference being that the resistance readings before and after cycling are always made at the ice point, 0 °C.

Zuzek showed the differences yielded by these three methods are quite significant, so the user should be clear which method is used when reporting results [Zuzek 2010].

4.8. **Reproducibility, or long-term stability**

Despite the relatively robust construction of IPRTs, they are still susceptible to strain in the platinum wire causing changes in electrical resistance, resulting in a shift of the $R(T)$ versus T relationship. Also, a change in the impurity concentration (and oxidation) affects the thermometric properties [Arai 1992, Berry 1982, Berry 1982b]. Therefore, the stability of PRTs should be tested with time during thermal cycling between extreme temperatures in the expected range of operation. For example, in reference [Mangum 1982] an investigation of 60 IPRTs from 5 manufacturers was performed to evaluate the stability upon thermal cycling. Most of the IPRTs exhibited calibration drifts, instability attributed to moisture, and hysteresis. After cycling to 235 °C, half of the thermometers showed changes in $R(0$ °C) larger than the equivalent of 15 mK, and a quarter showed changes larger than 50 mK. Comparable results were obtained in other experiments [Curtis 1982,

Berry 1982, Berry 1982b, Mangum 1982, Sinclair 1972]. More recent experiments (e.g. [Arai 1992, Crovini 1992]), on the other hand, found rather better behaviour. Most of the national standard specifications give tolerances for the permitted variation in resistance after a given number of thermal cycles.

Many experiments have been done, especially below 650 °C, to evaluate the long-term stability of IPRTs (the distinction between instability and hysteresis is slight, but the latter can be reversible). These have involved, in total, hundreds of thermometers and include models from most of the manufacturers. Most of the thermometers had $R(0\text{ °C}) = 100\ \Omega$, and most of the tests were in the range -50 °C to 250 °C . There was little uniformity in the results. Some thermometers were stable to within 5 mK, many to within 10 mK, and most to within 50 mK. Increasing the test range to 420 °C or higher did not significantly alter the results. In many PRTs exposed to high temperature, it was observed that, after an initial decrease in resistance, the drift rate became smaller after being well annealed. The final drifts in $R(0\text{ °C})$ are expected to range from 0.1 K to several kelvin, since the instability increases rapidly at higher temperature. Nevertheless, 5 sensors designed for use up to the gold point have shown, after an annealing at 1100 °C for a total of 250 hours, drifts of $R(0.01\text{ °C})$ smaller than 8 mK during the last 50 hours of annealing [Arai 1992]. Figures 4.8.1-4.8.7 show examples of instability in tests of various batches of thermometers. Up to 700 °C , results from Hahtela [Hahtela 2014], where the stability of both wire-wound and ceramic thin-film sensors were evaluated, the stability of all sensors was found to be of the order of 1 °C per year; in that study the wire-wound sensors were more stable than the thin-film ones.

A recent assessment of 20 ‘typical good’ thin-film IPRTs showed stability within $\pm 40\text{ mK}$ when cycled between -200 °C and 80 °C [Veltcheva 2018] and, remarkably, showed the restorative effect of leaving the IPRTs at room temperature for a few days which appears to allow the sensing element to ‘relax’ and regain its original resistance following cycling (Figure 4.8.7).

Sato [Sato 2013] showed that pre-annealing metal sheaths at 450 °C for 72 hours before assembly results in almost complete elimination of drift, presumably because this removes surface contaminants from the sheath. Subsequent drift tests at 450 °C revealed an initial sudden drop of a few mK, followed by a gradual rise in resistance over the following 1000 hours; in general the maximum drift amounted to less than 10 mK, with only two exceptions which exhibited a positive drift of almost 40 mK after 800 hours.

This is consistent with the findings of [Ljungblad 2013] who presented an extensive set of calibrations of sensors which had been used in the field and returned for calibration each year (calibrated between 0 °C and 500 °C), allowing assessment of drift of IPRTs which had undergone typical use. The drift of the IPRTs was generally less than $\pm 5\text{ mK}$ per year, with one exception which varied between about $\pm 20\text{ mK}$ per year.

Importantly, cycling of thin-film IPRTs used in sub-sea measurements between -30 °C and $+30\text{ °C}$ at least four times has been shown to minimise both drift and hysteresis when used over that temperature range [Veltcheva 2020].

Hashemian et al. [Hashemian 1990] have conducted an extensive set of IPRT aging studies on a set of 30 nuclear-grade IPRTs and 17 commercial-grade IPRTs. In this

context ‘commercial grade’ means those IPRTs that conformed to the ASTM E1137 specification at the time of the study. Since the study predated the advent of the IEC 62397 [IEC 62397] specification, the term ‘nuclear grade’ was specific to whatever additional performance requirements were placed on IPRTs purchased by nuclear plant operators and/or defined by the US Nuclear Regulatory Commission at that time. The IPRTs of both grades were subjected to nearly continuous thermal aging at 320 °C for a period of 18 months and periodically recalibrated. Certain subsets of those IPRTs were subjected to additional tests including vibration, humidity, high temperature and thermal cycling. High temperature testing was conducted at 400 °C for a duration of three days. Normal aging was observed within a ± 0.2 °C band of drift for 63 % of the IPRTs under study. The balance exhibited some degree of abnormally high drift and/or failure. It was observed that the drift behaviour of the nuclear grade IPRTs was about half the magnitude of the drift observed in the commercial PRTs.

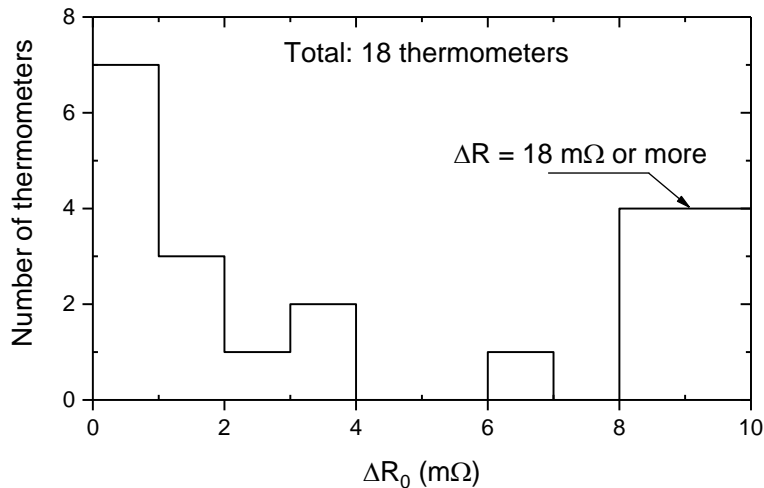


Figure 4.8.1. Histogram showing the shift in $R(0\text{ °C})$ after a single exposure to liquid oxygen following stabilisation at 450 °C for a group of 18 industrial platinum resistance thermometers having $R(0\text{ °C}) = 100\ \Omega$ [Sinclair 1972].

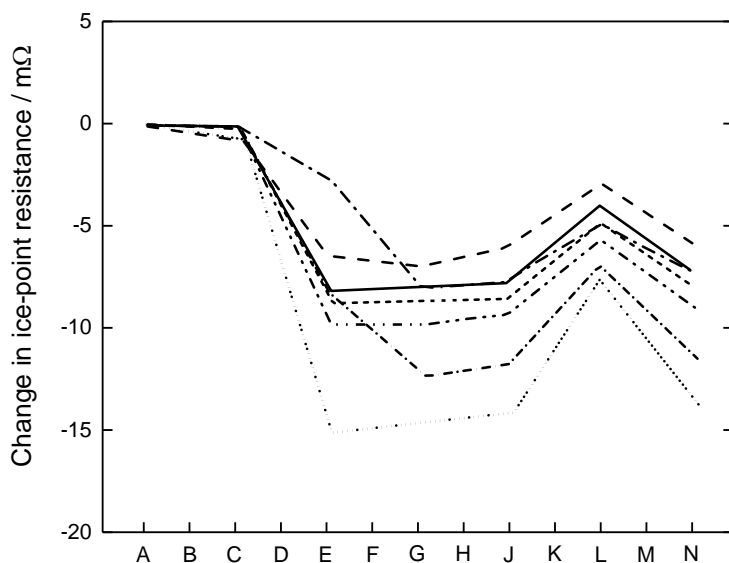


Figure 4.8.2. Changes in $R(0\text{ }^{\circ}\text{C})$ for seven IPRTs after 10 cycles between $20\text{ }^{\circ}\text{C}$ and $-196\text{ }^{\circ}\text{C}$ (with occasional measurement also of $R(100\text{ }^{\circ}\text{C})$). A) measurement of $R(0\text{ }^{\circ}\text{C})$; B) after measurement of $R(100\text{ }^{\circ}\text{C})$; C) Measurement of $R(0\text{ }^{\circ}\text{C})$; D) after ten cycles between 293 K and 77 K ; E) measurement of $R(0\text{ }^{\circ}\text{C})$; F) ten cycles between 293 K and 77 K ; G) measurement of $R(0\text{ }^{\circ}\text{C})$; H) ten cycles between 293 K and 77 K ; J) measurement of $R(0\text{ }^{\circ}\text{C})$; K) measurement of $R(100\text{ }^{\circ}\text{C})$; L) measurement of $R(0\text{ }^{\circ}\text{C})$; M) ten cycles between 293 K and 77 K ; N) measurement of $R(0\text{ }^{\circ}\text{C})$. After [Besley 1983].

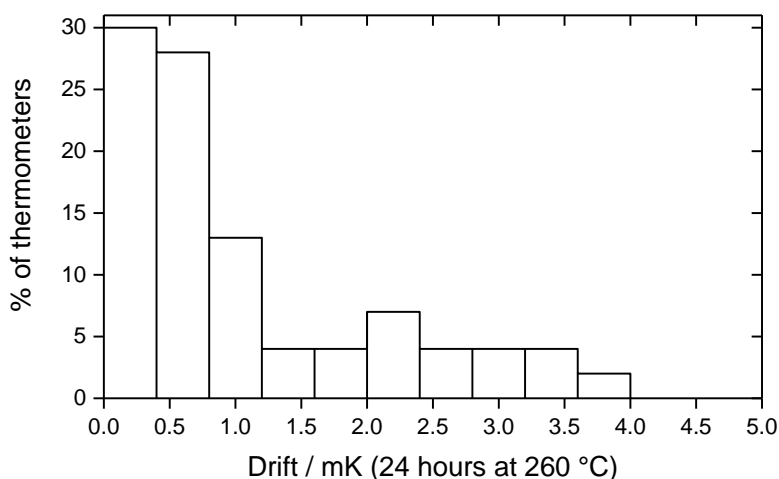


Figure 4.8.3. Distribution of the rate of drift of $R(0\text{ }^{\circ}\text{C})$ due to exposure to $260\text{ }^{\circ}\text{C}$ for up to 100 hours for a group of 87 IPRTs [Besley 1983].

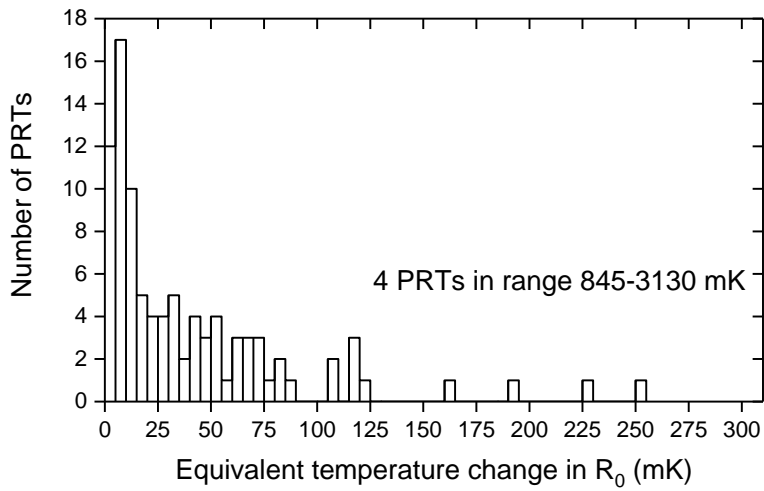


Figure 4.8.4. Histogram of the maximum equivalent temperature change in $R(0\text{ }^{\circ}\text{C})$ during ten 24-hour exposures to $235\text{ }^{\circ}\text{C}$ for a group of 98 IPRTs [Mangum 1984].

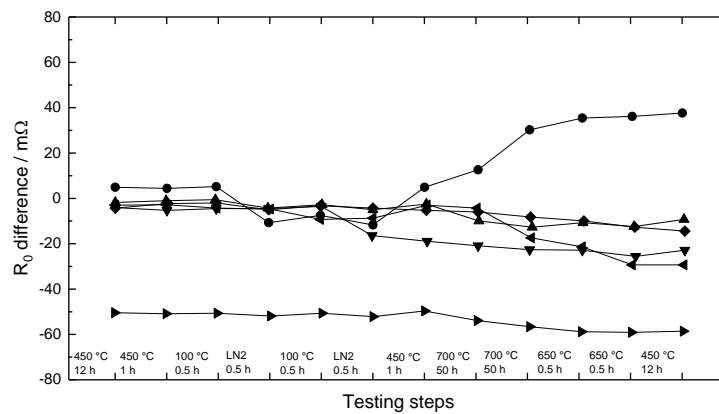


Figure 4.8.5. Changes of the ice-point resistance, R_0 , with respect to its initial value, resulting from the various thermal treatments from $-196\text{ }^{\circ}\text{C}$ (LN_2) to $700\text{ }^{\circ}\text{C}$. The 6 IPRTs of this figure are for use in the temperature range $0\text{ }^{\circ}\text{C}$ to $630\text{ }^{\circ}\text{C}$ ($40\text{ m}\Omega$ is equivalent to approximately $0.1\text{ }^{\circ}\text{C}$) [Crovini 1992].

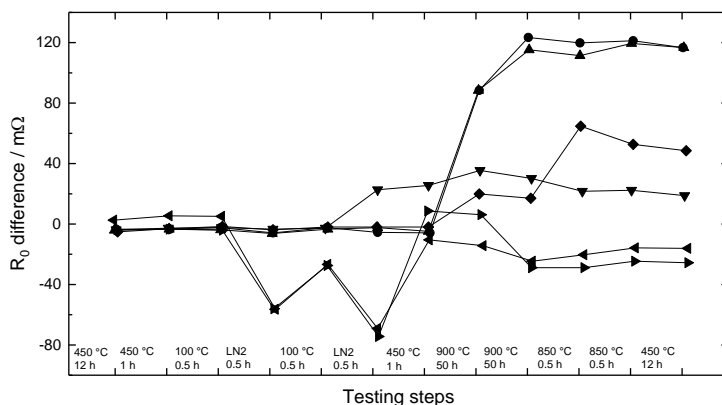


Figure 4.8.6. Changes of the ice-point resistance, R_0 , with respect to its initial value, resulting from the various thermal treatments from -196 °C (LN₂) to 900 °C . The 6 IPRTs of this figure are for use in the temperature range 0 °C to 850 °C ($40\text{ m}\Omega$ is equivalent to approximately 0.1 °C) [Crovini 1992].

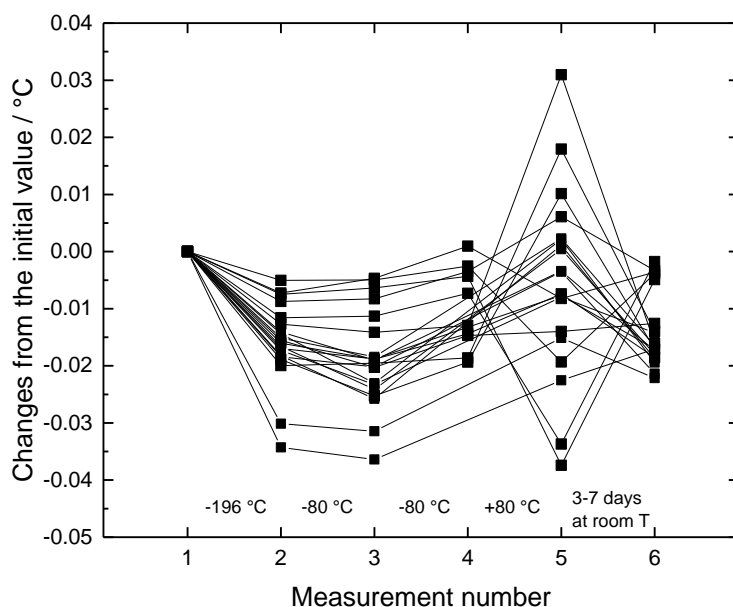


Figure 4.8.7. Changes in the indicated ice points of 20 film-type IPRTs during calibration. 1 Initial measurement, 2 after -196 °C , 3 after -80 °C , 4 repeat, 5 after 80 °C , 6 repeat after 3-7 days at room temperature (after [Veltcheva 2018]).

The oxidation of platinum and the reduction of PtO₂ as a function of temperature and oxygen partial pressure is a further important influencing quantity for the stability and interpolation uncertainty of IPRTs in the temperature range from 100 °C to 600 °C or higher. This affects thin-film IPRTs particularly, due to the

large surface area to volume ratio compared with wire-wound sensors. Experiments have been performed on the reduction of PtO₂ in different atmospheres [Jursic 2014]: notably, in air the main decomposition of PtO₂ begins at 595 °C which makes them highly susceptible to drift above this temperature.

4.9. Contamination

At temperatures above 250 °C platinum thermometers become progressively more susceptible to contamination [Nicholas 2001, p228]. The effect of the contaminants is to increase the impurities in the metal and hence increase the resistance (e.g. $R(0\text{ °C})$) and decrease the temperature coefficient, α . (Table 4.9.1). Further information may be found in [Davis 2001, Vines 1941]. If the level of impurities is high, the resulting departures from the reference tables can exceed several degrees, effectively destroying the thermometer. The damage is irreparable since, unlike crystal defects, the impurities cannot be removed by annealing the thermometer.

Probably the most common cause of contamination is the migration of iron, manganese, nickel and chromium from stainless steel and Inconel sheaths and insufficiently purified ceramic powder or carrier material. An overnight exposure of an unprotected ceramic element at 500 °C can easily cause several degrees error. The migration of contaminants can be reduced by heat-treating the sheaths in air or oxygen before the thermometer is assembled. This builds a layer of oxide, which is relatively impervious to metal atoms (and thin-film thermometers are often treated with a proprietary coating). The heat treatment can also drive off the lubricant used to draw the tube, another source of contamination. Other possibilities for improvement in performance include operating in air, i.e., the sheath is filled with air before it is closed, or the sheath is kept open, so that there is a permanent exchange of the atmosphere around the sensing element. This latter measure can be problematic if the sensor is operated in air at temperatures below the dew point, so the envisaged application needs to be kept in mind when considering this.

The coefficient values shown in Table 4.9.1 are taken from an industrial handbook [ABB 2013] and are essentially equivalent to those as originally published by Cochrane [Cochrane 1972]. It should be noted that different values for these coefficients may be found elsewhere in the literature [Rhys 1969], some of which are highly discrepant. The coefficients' uncertainties, while generally unknown, are probably no better than 10 %.

Table 4.9.1. Effect of contamination on the temperature coefficient (α) of platinum expressed as a proportionality to the mass fraction of the impurity in parts per million (ppm, or $\mu\text{g/g}$) [ABB 2013].

| Element | $d\alpha / 10^{-6} \text{ ppm}^{-1}$ |
|---------|--------------------------------------|
| Fe | -1.28 |
| Ni | -0.16 |
| Ir | -0.20 |
| Mn | -0.21 |
| Rh | -0.09 |
| Cu | -0.35 |
| Pd | -0.10 |
| Ag | -0.15 |
| Au | -0.07 |
| Pb | -0.90 |
| Cr | -3.25 |

4.10. Electromagnetic interference

Electromagnetic interference (EMI) is any unwanted voltage or current that originates from outside the measurement circuit [Nicholas 2001, p234]. Sources of EMI include electric motors, transformers, power cables, radio and TV transmissions, leakage currents from electric heaters, and ground loops. Some examples are shown in Figure 4.10.1.

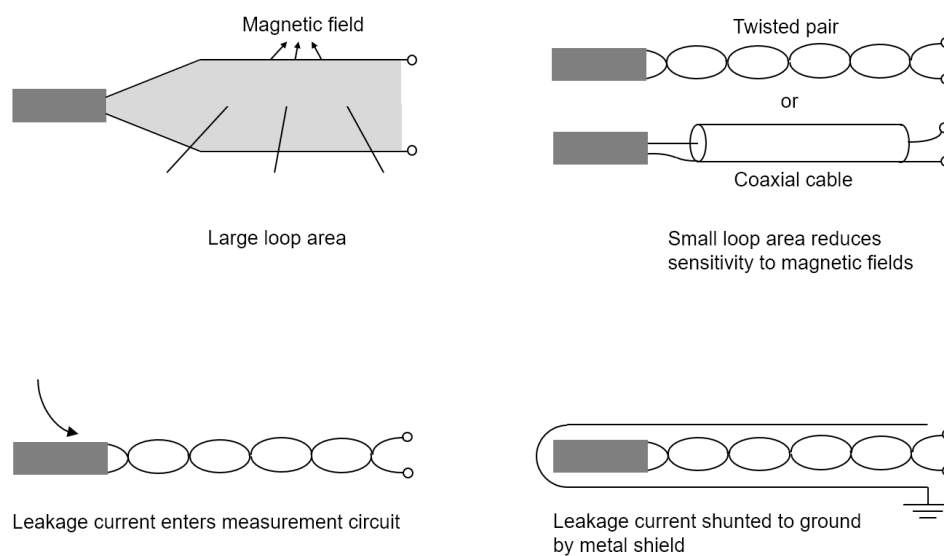


Figure 4.10.1. Examples of measurement practices which are susceptible to EMI (left), and relatively immune to EMI (right). After [Nicholas 2001].

For many applications, EMI due to magnetic fields can be reduced by metal screens. However, for thermometry a metal screen must be several metres thick to have a significant effect on the field at DC and the lower frequencies used in resistance thermometry. There are two basic techniques for reducing magnetic EMI. Firstly, the EMI source and the thermometer should be separated as much as

possible. This exploits the fact that the coupling between the source and the thermometer falls off as the distance cubed. Secondly, all lead wires should be kept as close together as possible. Twisted pair and coaxial cables are very effective in reducing the loop area exposed to magnetic fields.

5. Calibration

A calibration is needed if compliance with a stated tolerance is not sufficient for the required purpose. It enables a user to obtain a more accurate temperature measurement that is traceable to the ITS-90. Certificates of calibration or traceability are often supplied with thermometers, but periodic checks must be made to verify the validity of the certification. A calibration consists of the measurement of the resistance of the thermometer at multiple temperatures distributed over the calibration range, which permits the generation of an interpolating function. A certificate of calibration accompanying the IPRT presents the results of the calibration, the associated uncertainties, and other relevant information. Calibrations are usually undertaken under closely controlled laboratory conditions and the uncertainties are correspondingly smaller than those which apply in subsequent use of the IPRT, which includes the calibration uncertainties as a component.

5.1. Methods

The calibration of a resistance thermometer requires the resistance to be measured at a series of known temperatures. These known temperatures can be obtained in fixed-point apparatus, as for SPRTs in the ITS-90, or in a comparison apparatus where the temperature is measured by a calibrated SPRT. In practice, IPRTs are usually calibrated by comparison, in apparatus that can provide suitable temperature control and uniformity, such as a fluid bath from $-80\text{ }^{\circ}\text{C}$ up to about $280\text{ }^{\circ}\text{C}$, and a furnace at higher temperatures, or a ‘dry block calibrator’ (a temperature controlled metal block).

At lower temperatures, a cryostat is needed. A comparator for the calibration of IPRTs in the temperature range from $-190\text{ }^{\circ}\text{C}$ to $-25\text{ }^{\circ}\text{C}$ has been described by Bosma [Bosma 2013] which can yield calibration uncertainties of less than 5 mK over this range.

The number of calibration points needed depends upon the temperature range and uncertainty required. A wider range or a lower uncertainty is likely to require a more complex interpolation equation and a larger number of calibration points. As a general guide, the number of points should be at least twice the degree of the interpolation function.

5.2. Equations

In principle, any of the equations used for SPRTs can also be used with IPRTs, although within some (generally unknown) broader limits of accuracy, more due to the construction of the IPRT sensor, that generally is not completely strain-free, than to the purity of the platinum of the sensor. It should be remembered that the techniques described here have been tested for sensors designed for the purpose (in a metal sheath, long enough to provide the necessary immersion, see Section 4.2) or mounted by the experimenters in suitable glass or metal sheaths. Rugged sheaths or thermowells meant for industrial applications should be removed before calibration.

The Callendar-Van Dusen equation (Section 2.2), used until 1968 for both IPRTs and SPRTs, is still used in the IEC and ASTM standards for the IPRTs because the specified tolerances in most cases are larger than the systematic differences between the CVD equations and the ITS-90. These systematic differences can be obtained from a comparison of the ITS-90 reference function with the standardised CVD equations, see Figure 5.2.1. The ITS-90 interpolation, using deviation functions, can nevertheless be used for IPRTs, even though IPRTs do not comply with the ITS-90 criteria (in which the effective α value should be $> 0.003925 \text{ }^\circ\text{C}^{-1}$). Unique solutions to the ITS-90 deviation equations are obtained with just one to three calibration points, depending on the number of required coefficients for a given calibration subrange. However, where uncertainties of $< 0.01 \text{ }^\circ\text{C}$ are required, one or more additional calibration measurements should be included to verify the interpolation.

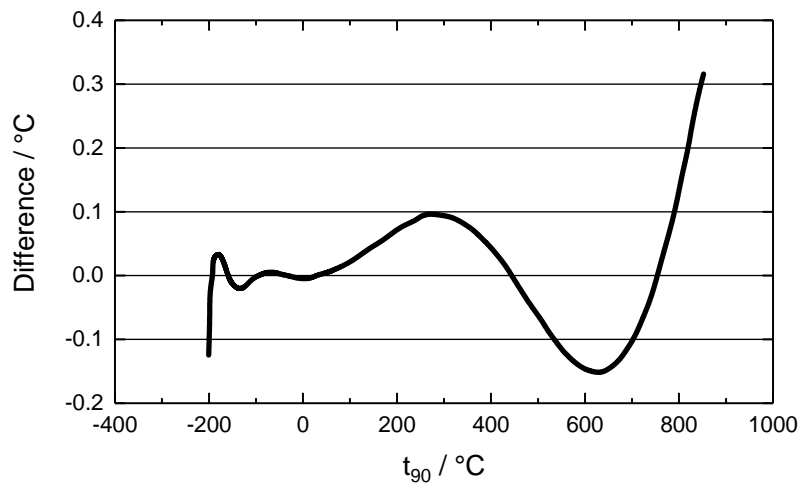


Figure 5.2.1. Differences between the standardised CVD equations and the ITS-90 in the temperature range from $-200 \text{ }^\circ\text{C}$ to $850 \text{ }^\circ\text{C}$ (after [Marcarino 2004b]).

If the standard CVD coefficients are recalculated for an individual sensor, using calibration data in temperature ranges between $-80 \text{ }^\circ\text{C}$ and $660 \text{ }^\circ\text{C}$, where most IPRTs are used, the systematic differences between the CVD equations and the ITS-90 are significantly smaller [Marcarino 2001].

As described, these differences are well within the specified tolerances of the IEC and ASTM standards. Nevertheless, many IPRTs exhibit stabilities at the 10 mK level. Therefore, there is an increasing demand for calibrations of IPRTs to the same level of uncertainty. The CVD equations allow this uncertainty level only in the range from $0 \text{ }^\circ\text{C}$ to $250 \text{ }^\circ\text{C}$. For use in other temperature ranges, different interpolation equations are required. The degree of complexity of the interpolation equations depends on the temperature range and on the measurement precision needed by the user.

5.2.1. Polynomial functions

The use of simple polynomial functions as interpolating equations, relating the resistance, $R(t_{90})$ or ratios $W(t_{90})$ to t_{90} to approximate the ITS-90, have been examined over various temperature ranges using least squares techniques [Connolly 1992, Hashemian 1992, Zhang 1992]. Connolly found approximations to the ITS-90 within ± 0.001 °C with a cubic function in the range 0 °C to 250 °C, within ± 0.002 °C with a quartic function in the range 0 °C to 400 °C, and within ± 0.005 °C with a quartic function in the range 0 °C to 500 °C [Connolly 1992]. (See also Section 5.3.1.)

Low-order polynomial functions can also be useful for interpolation between calibration differences for thermometers with digital readouts, or for the corrections to be applied to the readings (see Section 5.3.2).

5.2.2. CVD function

The use of the Callendar-Van Dusen function as an interpolation equation to approximate to the ITS-90 was examined between -200 °C and 850 °C by several researchers [Cimerman 1999, Marcarino 2001, Zhang 1992, Kaiser 1999, Marcarino 2004, Mendez-Lango 2001, Crovini 1992]. All authors achieved similar results.

However, there is no reason to suppose that the CVD equation is better than simple empirical polynomial functions of a similar degree, and it is less convenient in that it takes two steps to calculate the three coefficients. Moreover, a polynomial expressing temperature as a function of resistance can be directly solved for temperature by inserting a measured value of resistance, whereas the CVD equation cannot. It has recently been suggested that the CVD equation is technically obsolete and should be phased out [Veltcheva 2018].

5.2.3. Direct use of the ITS-90 interpolation for IPRTs

Interpolation can also be obtained by applying the ITS-90 relations to IPRTs [Mendez-Lango 2001, Tamura 1992, Moiseeva 2002]. This technique is possible because no systematic differences (> 0.01 °C) appear among platinum resistance thermometers with different α , ranging from $3.9244 \cdot 10^{-3}$ °C⁻¹ to $3.85 \cdot 10^{-3}$ °C⁻¹ [Kaiser 1999, Marcarino 2004, Mendez-Lango 2001, Tamura 1992, Moiseeva 2002]. Therefore, it should be possible to use the ITS-90 equations to interpolate between IPRT calibration data with an accuracy within the range -80 °C to 650 °C of better than ± 0.01 °C. Generally, the limitation in the accuracy of an IPRT is not due to the interpolation of the calibration data with the ITS-90 equations, but to the stability of the sensor that, in general, is not strain-free. Following these considerations, in 2003 the CCT made the recommendation [CCT/03-14] that:

“WG2 encourages use of the ITS-90 interpolation scheme with IPRTs, particularly since many of the electronic readouts (digital thermometers) already support this capability. The use of IEC-751 with the standard IEC coefficients is satisfactory if an uncertainty of ± 0.2 K is sufficient. However, the ITS-90 interpolation scheme has been shown to afford interpolation

accuracies within 10 mK when applied to IPRTs and this result also appears to be independent of α (sensitivity).”

Recent data e.g. [Yamazawa 2011, Fericola 2008, Yang 2015] support the above observations. Overall, ITS-90 interpolations have greater credibility than the other approaches, based on the evidence in [Tamura 1992, Fericola 2008, Dubbeldam 1998, Hill 2008, Veltcheva 2018]. The CVD equation, with constants A , B and C derived from a calibration of the individual sensor, can only give similar accuracies over limited temperature ranges, and additional data (check-points) should be used to verify the interpolation accuracy. Higher-order least-squares fits to the calibration data can do better, and both these alternatives have simpler mathematical formulations than those of the ITS-90.

5.3. Examples of processing IPRT calibration data, and uncertainties

5.3.1. Example of interpolation

Interpolation methods and uncertainty estimation are outlined using data from two examples⁵. In the first, a Pt100 sensor has been calibrated at 7 temperatures in the range from $-40\text{ }^{\circ}\text{C}$ to $155\text{ }^{\circ}\text{C}$. The temperature and resistance data are presented in chronological order in Table 5.3.1. A measurement was first made in a water triple point cell, and this was repeated at various times in the calibration, showing the repeatability of the sensor on temperature cycling. Other measurements were made in calibration baths by comparison with two calibrated SPRT standards. At each temperature, two or three sets of comparisons were made, and the results given are the averages of the temperatures from the SPRTs and the thermometer resistances.

Table 5.3.1. Temperature and resistance data for a Pt100 calibration.

| Point no | Temperature $t / ^{\circ}\text{C}$ | Resistance R / ohm | $t(\text{fit})$ (cubic) $^{\circ}\text{C}$ | $t(\text{fit}) - t(\text{data})$ mK | $R(\text{CVD})$ ohm | $\text{CVD} - \text{data}$ mK | $\text{CVD} - \text{cubic}$ mK |
|----------|---------------------------------------|--------------------------------|--|---|---------------------------------|---|--|
| 1 | 0.0100 | 99.96530 | 0.0150 | 4.99 | 99.96308 | 5.77 | 0.78 |
| 2 | -19.5244 | 92.32611 | -19.5242 | 0.13 | 92.32750 | -3.60 | -3.73 |
| 3 | -40.3004 | 84.15173 | -40.3010 | -0.63 | 84.15173 | 0.00 | 0.63 |
| 4 | 0.0100 | 99.96280 | 0.0086 | -1.42 | 99.96308 | -0.73 | 0.69 |
| 5 | 29.8655 | 111.54535 | 29.8631 | -2.39 | 111.54493 | 1.09 | 3.48 |
| 6 | 69.9975 | 126.94755 | 69.9975 | 0.05 | 126.94755 | 0.00 | -0.04 |
| 7 | 0.0100 | 99.96372 | 0.0109 | 0.95 | 99.96308 | 1.67 | 0.73 |
| 8 | 129.8212 | 149.55386 | 129.8225 | 1.34 | 149.55492 | -2.75 | -4.09 |
| 9 | 155.2482 | 159.03583 | 155.2476 | -0.65 | 159.03583 | 0.00 | 0.64 |
| 10 | 0.0100 | 99.96272 | 0.0084 | -1.62 | 99.96308 | -0.93 | 0.69 |

The first method used in processing the results was to do a least-squares fit to all the data, expressing the temperature as a function of resistance. A quadratic fit showed residuals $t(\text{fit}) - t(\text{data})$, being the differences between the fitted curve and

⁵ Further examples may be found in [Nicholas 2001].

the data, of up to 6.3 mK. This is not bad, but a cubic fit was nevertheless preferred, the largest residual being 2.4 mK, in Column 5 of Table 5.3.1, except at the first triple point measurement. The equation is (approximately):

$$t/^{\circ}\text{C} = -246.6585 + 2.37430R + 8.8611 \cdot 10^{-4}R^2 + 4.71085 \cdot 10^{-7}R^3 \quad (5.2.1)$$

Note that this form of equation, $t = f(R)$, is used because it is then simple to calculate temperatures from measured values of resistance. A cubic fit to an equation expressing the resistance as a function of temperature is just as good but is less convenient to use.

The residuals of the fit are used to estimate the statistical (Type A) uncertainty of the calibration: the standard deviation, u_A is

$$u_A = \sqrt{\frac{\sum_{i=1}^N (t_{fit} - t_{data})_i^2}{(N-n)}} \quad (5.2.2)$$

where N is the number of inputs (data points) and n is the number of output parameters (coefficients). With a cubic fit to the 10 points in Table 5.3.1, this gives is $u_A = 2.5$ mK. However, measurements were in fact made at only 7 distinct temperatures, the triple point of water having been measured four times, and the points are not properly distributed. A more realistic estimate of u_A in the whole range is obtained if the triple-point resistances are averaged: the standard deviation for the 7 distinct points is then 1.6 mK.

The second interpolation method was to use the CVD equation (see also Sections 2.4 and 7):

$$R(t) = R(0^{\circ}\text{C})[1 + At + Bt^2 + C(t - 100^{\circ}\text{C})t^3] \quad (5.2.3)$$

The first step in this procedure is to solve the quadratic part for the range above 0°C (where $C = 0$), and hence deduce A and B . This was done using the data at 0.01°C , 70°C and 155°C (a least-squares quadratic fit to all the data above 0°C was also done and gave a very similar result). The quadratic equation is:

$$R(t) = 99.95918 + 0.3969t - 5.903 \cdot 10^{-5}t^2 \quad (5.2.4)$$

where the leading term is the interpolated value of resistance at $t = 0^{\circ}\text{C}$. The equation can be simply rewritten in the CVD form:

$$R(t) = 99.95918[1 + 3.8985 \cdot 10^{-3}t - 5.905 \cdot 10^{-7}t^2] \quad (5.2.5)$$

The next step is to calculate C . This follows directly by rearranging the CVD equation and calculating the quantity $Q = R(t) / R(0 \text{ }^\circ\text{C}) - [1 + At + Bt^2]$, using values of $R(0 \text{ }^\circ\text{C})$, A and B as already determined, and the data at $-40 \text{ }^\circ\text{C}$ for the values of $R(t)$ and t . We then have $C = Q / (t - 100) t^3 = -7.378 \cdot 10^{-12}$.

Figure 5.3.1 shows the residuals of the quadratic and cubic fits, and also the differences between the CVD equation and the cubic fit.

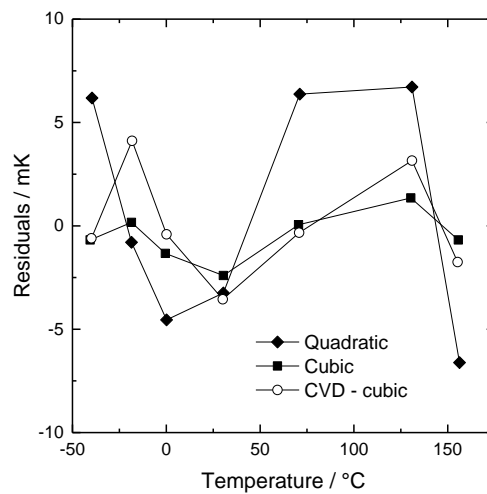


Figure 5.3.1. Residuals for quadratic (diamonds) and cubic (squares) fits of t as a function of R , in mK. The open circles are the differences between the CVD equation and the cubic fit.

Some points about the procedures should be noted:

- The methods can be used for any data, above and/or below $0 \text{ }^\circ\text{C}$, where compliance with IEC 60751 is not good enough and a specific calibration has been done. Clearly the quality of the fits will depend on the quality and distribution of the data, the temperature range, and the stability of the sensor.
- Over short ranges a quadratic fit may be adequate.
- For these data the cubic fit is a more satisfactory outcome: data at seven temperature points are used to determine four coefficients, leaving three ‘degrees of freedom’, and good statistics (a standard deviation of about 2 mK) are obtained.
- Note especially that fits should not be extrapolated outside the range of the data used.
- In this example, there is evidence of a lack of repeatability of the sensor, the first measurement at the triple point of water being significantly

different from the rest, and this will have compromised the quality of the fits.

- It must be expected that the fits, like the thermometer stability, will be less good for calibrations extending over wider ranges. More data will be needed to characterise the resistance accurately, and this will allow quartic or even higher order fits to be used, if necessary. However, care must be taken to avoid ‘over fitting’ which may introduce erratic behaviour in the curve: good practice in curve fitting, such as proper spacing of the data, must be observed.
- The CVD equation is less satisfactory overall but may nevertheless be adequate.
- If a CVD solution is to be used over wider ranges, it is more desirable that the coefficients A and B are determined from a least-squares fit. The value of C is then optimised to match the calibration data below 0 °C.
- For temperature ranges extending down to –40 °C it may be acceptable to set $C = 0$ in the CVD equation, i.e. to fit the full range using the quadratic function.
- Note that in the example given above, the values of A , B and C are of similar magnitudes to those in the standard IEC 60751, because all IPRTs have similar characteristics. However, the ‘standard’ values should only be used with uncertainties given by the tolerances in Tables 2.4.2 and 2.4.3, unless specific calibration checks are made.
- See White and Saunders [White 2007] for further information regarding uncertainties in calibration equations.

5.3.2. Example 2: Calibration of a direct reading temperature indicator with two IPRT probes

The second example concerns the calibration of two IPRT probes and a direct-reading digital temperature indicator, with a resolution of 0.001 °C. They were jointly calibrated from 10 °C to 30 °C by comparison against two standard platinum resistance thermometers in a temperature-controlled stirred oil bath.

Table 5.3.2 shows a possible uncertainty budget for the calibration (all contributions are expressed as standard uncertainties, coverage factor $k = 1$, i.e. coverage probability of 67 %). The list may not be comprehensive, and the numerical values are for illustration only.

Table 5.3.2: Uncertainty budget for the calibration of the IPRTs and indicator

| Temperature: 10 °C to 30 °C Source of uncertainty | Estimate ± | Unit | Probability distribution | Divisor | Sensitivity (°C / unit) | Uncertainty (k=1) (°C) |
|--|---------------|------|-----------------------------|---------|----------------------------|---------------------------|
| Type A | | | | | | |
| A01: repeatability of comparisons | not used | °C | | | | 0.0 |
| A02. Interpolation of differences | 0.0020 | °C | Normal | 1.00 | 1 | 0.0020 |
| Type B | | | | | | |
| Measurement uncertainties | | | | | | |
| B01. Resolution of indicator | 0.0005 | °C | Rectangular | 1.73 | 1 | 0.0003 |
| B02. PRT self-heating | not used | °C | Rectangular | 1.73 | 1 | 0.0 |
| B03. SPRT bridge linearity | 1.00E-05 | Ω | Rectangular | 1.73 | 10.3 | 0.0001 |
| B04. Calibration of SPRTs | 0.001 | °C | Normal | 2 | 1 | 0.0005 |
| B05. Drift in SPRTs since calibration | 0.001 | °C | Rectangular | 1.73 | 1 | 0.0006 |
| B06. Value of Std Resistor Rs | 0.10 | ppm | Normal | 2 | 0.0003 | 0.0000 |
| B07. Stability of Rs temperature | 0.01 | °C | Rectangular | 1.73 | 0.0005 | 0.0000 |
| B08. PRT stability and hysteresis | 0.002 | °C | Rectangular | 1.73 | 1 | 0.0012 |
| B09. TPW propagation in SPRTs | 0.0002 | °C | Normal | 2 | 1.13 | 0.0001 |
| Thermal conditions | | | | | | |
| B10. Bath uniformity | 0.002 | °C | Rectangular | 1.73 | 1 | 0.0012 |
| B11. Bath stability | 0.001 | °C | Rectangular | 1.73 | 1 | 0.0006 |
| B12. Stem conduction / immersion | 0.001 | °C | Rectangular | 1.73 | 1 | 0.0006 |
| Combined Type B | | | | | | |
| | | | | | | 0.0020 |
| Combined uncertainty (A and B) | | | | | | 0.0028 |
| Expanded uncertainty (k=2) | | | | | | 0.0057 |

Explanatory notes.

- A01: Repeatability of comparisons: in this example the statistical repeatability of the readings was less than the resolution of the indicator, and therefore it could not be determined. In such cases, the uncertainty of the reading is covered by Component B01 (resolution of the indicator).
- A02: Interpolation of differences: a statistical (Type A) uncertainty is derived from the standard deviation of the residuals of the (linear) least-squares interpolation of $t(\text{indicated}) - t(\text{bath})$ as a function of $t(\text{bath})$.
- B01: Resolution of PRT indicator: this is half the instrument discrimination, i.e. half the least significant digit of the readout display.
- B02: PRT self-heating: this was not determined for the fixed-current indicator. The calibration applies at the current used.
- B03: SPRT bridge linearity: from periodic bridge checks. The sensitivity factor, $10.3 \text{ } ^\circ\text{C}/\Omega$, converts the uncertainty in resistance to the equivalent in $^\circ\text{C}$.
- B04: Calibration of reference SPRTs: this is taken from the SPRT calibration certificates, at $k = 2$.
- B05: Drift in SPRTs since last calibration: this is estimated from measurements of $R(0.01 \text{ } ^\circ\text{C})$ and prior performance of the SPRTs.
- B06: Value of standard resistor, R_s , used with the SPRTs: from the certificate. The sensitivity factor is the inverse of the PRT temperature coefficient, $\sim 4000 \text{ ppm}/^\circ\text{C}$.

- B07: Stability of R_s during comparisons: from its temperature coefficient and temperature control stability. The sensitivity factor is the ratio of the temperature coefficient of R_s (<2 ppm/°C) to that of the PRT.
- B08: PRT stability and hysteresis: this is estimated using check points to determine the changes in the readings at 0 °C and at mid-range.
- B09: TPW propagation in SPRTs: from the uncertainty in TPW measurements and the TPW propagation factor, which is 1.13 at 30 °C.
- B10: Bath uniformity: this is estimated from prior measurements of the bath temperature uniformity.
- B11: Bath stability: this is estimated by monitoring the bath temperature over a period of time.
- B12: Stem conduction / immersion: this is estimated from tests in which the PRT immersion is changed.

In this budget the combined standard uncertainty of the measurements (excluding interpolation) is 0.0020 °C. Including the interpolation, this rises to 0.0028 °C. The expanded uncertainty U ($k = 2$), with a coverage probability of 95 %, is reported in the certificate as 0.006 °C. The calibration certificate is shown in Figure 5.3.2. Note that for clarity this presents the results as corrections to be added to the readings, rather than its negative, the calibration differences.



Cal O'Bration Labs Ltd

1 Really Close, Teddington, United Kingdom TW11 0LW
Tel: +44 20 8977 0000 Fax: +44 20 8977 0001



Certificate of Calibration

FOR: ACME Industries Ltd
10 West Close
Easton
BN1 1NB

For the attention of: Mr John Smith

DESCRIPTION: ACME 50 digital indicator with two associated probes
Measurement resolution 0.001 °C

IDENTIFICATION: ACME 50 serial number 747-400
Probe serial number A350a
Probe serial number A350b

DATE OF CALIBRATION: 7 July 2020

MEASUREMENTS

The ACME 50 digital indicator and associated probes were submitted for calibration between 10 °C and 30 °C in terms of the International Temperature Scale of 1990.

The probes were immersed to a depth of approximately 180 mm in a well-stirred liquid bath. The combined unit was calibrated by comparison of the displayed temperatures with those of the Laboratory reference thermometers and the results given apply to the combined performance.

Linear interpolation equations were derived for interpolating the calibration corrections to be applied to the readings

Throughout the calibration the ambient temperature was about 20 °C.

UNCERTAINTY

The temperature of the stirred liquid-bath was measured by the Laboratory reference thermometers with an estimated uncertainty of 0.002 °C. The expanded uncertainty of calibration, at the time of test is 0.006 °C. This includes all uncertainties in the measurements and in realising the calibration temperatures, and in the interpolation of the corrections. It is based on a standard uncertainty multiplied by a coverage factor $k = 2$, providing a coverage probability of approximately 95%. The uncertainty evaluation has been carried out in accordance with UKAS requirements.

Reference: 2020123456/1/XYZ

Date of issue: 7 July 2020

Checked by:

Signed:

Name: Dr J Doe on behalf of Cal O'Bration Labs

Page 1 of 2

(Authorised Signatory)

Figure 5.3.2a. Calibration certificate for digital temperature indicator and IPRT (page 1).

Cal O'Bration Labs Ltd

Continuation Sheet

RESULTS

The results of the test are set out in the following tables, where the corrections to obtain the ITS-90 temperature are stated to the nearest 0.001 °C and represent the mean of the observations. To obtain the correct temperature the appropriate correction from the calibration table should be added to the reading, with due regard to the sign.

| Temperature, t_{90} / °C | Thermometer corrections / °C | |
|-------------------------------|------------------------------|--------|
| | A350a | A350b |
| 10.01 | 0.001 | -0.035 |
| 15.01 | -0.013 | -0.049 |
| 20.00 | -0.031 | -0.071 |
| 25.00 | -0.042 | -0.087 |
| 29.99 | -0.061 | -0.103 |

The equations to be used for calculating the corrections at temperatures t in the range between 10 °C and 30 °C are:

Probe A350a: Correction / °C = $-0.00306 t / °C + 0.0320$

Probe A350b: Correction / °C = $-0.00348 t / °C + 0.0006$

The results given in this certificate relate only to the items calibrated.

Reference: 2020123456/1/XYZ
Checked by:

Page 2 of 2

Figure 5.3.2b. Calibration certificate for digital temperature indicator and IPRT (page 2).

6. Conclusions and further reading

In this guide some key aspects of manufacture, selection and use of IPRTs have been described, but it is by no means comprehensive. Furthermore, best practice is continuously improving as more work is carried out to understand the metrological characteristics of IPRTs, and as IPRT manufacturing techniques improve.

It is important to bear in mind that the thermometer is only part of the measurement solution: care must be taken to ensure that the other aspects of the measurement set-up are fit for purpose, in particular with respect to the three modes of heat transfer, namely conduction (e.g. immersion), convection (adequate thermal contact with liquids or gases), and thermal radiation.

The interested reader may wish to consider some of the books which contain useful information on IPRTs and guidance appropriate to their practical use, including:

- J.V. Nicholas, D.R. White, Traceable Temperatures [Nicholas 2001]
- L. Michalski, K. Eckersdorf, J. Kucharski, J. McGhee, Temperature Measurement [Michalski 2001]
- R.E. Bentley, Handbook of Temperature Measurement series (in particular [Bentley 1998])
- T.J. Quinn, Temperature [Quinn 1990]
- P.R.N. Childs, Practical Temperature Measurement [Childs 2001]

7. Appendix 1: The original and modern Callendar-Van Dusen equations

In developing the platinum resistance thermometer in the late nineteenth century, Callendar showed that the characteristic is quite well described by a quadratic temperature dependence, and he devised two parameters, α and δ , to describe this. The addition of a third parameter, β , was proposed in 1925 by Van Dusen to improve the accuracy below 0 °C. The resulting Callendar-Van Dusen (CVD) equation in its original form related the temperature, $t/^\circ\text{C}$, to the resistance ratio, $W(t) = R(t) / R(0\text{ }^\circ\text{C})$, as follows:

$$t = \frac{1}{\alpha} (W(t) - 1) + \delta \left(\frac{t}{100\text{ }^\circ\text{C}} \right) \left(\frac{t}{100\text{ }^\circ\text{C}} - 1 \right) + \beta \left(\frac{t}{100\text{ }^\circ\text{C}} - 1 \right) \left(\frac{t}{100\text{ }^\circ\text{C}} \right)^3 \quad (\text{A1.1})$$

where $\beta = 0$ for $t > 0\text{ }^\circ\text{C}$. Solving this at $t = 100\text{ }^\circ\text{C}$ leads to:

$$\alpha = \frac{\{W(100\text{ }^\circ\text{C})-1\}}{100} = \frac{\{R(100\text{ }^\circ\text{C})-R(0\text{ }^\circ\text{C})\}}{100 R(0\text{ }^\circ\text{C})} \quad (\text{A1.2})$$

Thus α is the mean temperature coefficient of normalised resistance between 0 °C and 100 °C, and it was determined from measurements at the ice and steam points. The second parameter δ was then determined from a further measurement, originally specified in the ITS-27 as the boiling point of sulphur (~444 °C). The additional term in β for the range below 0 °C was chosen in such a way that the full CVD equation is continuous in value and first and second derivatives at 0 °C. β was determined from a low temperature measurement, for which the boiling point of oxygen was specified, though in practice the lowest calibration point would usually be chosen.

It is clear that in this form the parameters can conveniently be determined one after the other (using mechanical calculators), but in modern times it has become usual to write the equation as:

$$R(t) = R(0\text{ }^\circ\text{C})[1 + At + Bt^2 + C(t - 100\text{ }^\circ\text{C})t^3] \quad (\text{A1.3})$$

in which $C = 0$ for $t > 0\text{ }^\circ\text{C}$, and there are exact relationships between the two sets of parameters:

$$A = \alpha (1 + \delta/100\text{ }^\circ\text{C})\text{ }^\circ\text{C}^{-1}, B = -10^{-4} \alpha \delta\text{ }^\circ\text{C}^{-2}, C = -10^{-8} \alpha \beta\text{ }^\circ\text{C}^{-4} \quad (\text{A1.4})$$

Equation (A1.3) is how the equation appears in IEC 60751, with standard values for A , B and C , of

$$A = 3.9083 \cdot 10^{-3}\text{ }^\circ\text{C}^{-1}, B = -5.775 \cdot 10^{-7}\text{ }^\circ\text{C}^{-1}, C = -4.183 \cdot 10^{-12}\text{ }^\circ\text{C}^{-4} \quad (\text{A1.5})$$

Resistances are tabulated at intervals of 1 °C for a sensor of $R(0\text{ °C}) = 100\ \Omega$.

To determine the CVD coefficients for a particular thermometer, the first step is to derive the constants A and B in the quadratic $R(t\text{ °C}) = R(0\text{ °C})[1 + At + Bt^2]$ from measurements at (or near) 0 °C and at two higher temperatures. More points can usefully provide checks of the interpolation, or least-squares regression can be used. In that case, the lead term in a fit of $R = f(t)$ is the interpolated value of the resistance ratio at 0 °C, and the equation can be divided by this quantity to arrive at the values of A and B (this is convenient if the triple-point of water is used instead of the ice point).

The next step is to take a calibration point $(R(t), t)$ below 0 °C to determine C . Since A , B and the value of $R(0\text{ °C})$ are already known, C can be calculated by direct substitution. Again, an additional point will provide a check of the interpolation.

Further guidance on interpolation of calibration data is given in Section 5.2.

8. References

- [ABB 2013] ABB Automation Products GmbH, 2013 Industrial Temperature Measurement – Basics and Practice, https://library.e.abb.com/public/bc79d6844ab746809f1930b61656c791/03_TEMP_EN_E02.pdf
- [Actis 1982] Actis, A., Crovini, L., 1982 Interpolating Equations for Industrial Platinum Resistance Thermometers in the Temperature Range from -200 °C to +420 °C; *Temperature: Its Measurement and Control in Science and Industry* (American Institute of Physics, New York) 5, 819-827
- [Arai 1992] Arai, M., and Sakurai, H., 1992 Development of industrial platinum resistance sensors for use up to the gold point; *Temperature: Its Measurement and Control in Science and Industry* (American Institute of Physics, New York) 6, 439-442
- [ASTM E1137] ASTM E1137 / E1137M – 08 (2020), Standard Specification for Industrial Platinum Resistance Thermometers (ASTM International, West Conshohocken, PA, 2020).
- [ASTM E563] ASTM E563 - 11(2016) Standard Practice for Preparation and Use of an Ice-Point Bath as a Reference Temperature (ASTM International, West Conshohocken, PA, 2004).
- [ASTM E644] ASTM Standard E644, in *Standard Test Methods for Testing Industrial Resistance Thermometers* (ASTM International, West Conshohocken, PA, 2004). DOI: 10.1520/E0644-04, www.astm.org
- [Ballico 2014] Ballico, M.J., Sukkar, D. 2014 Temperature Dependence of IPRT and SPRT Self-Heating: Does Working with W Really Help? *Int. J. Thermophys.* 35:1067-1076
- [Bass 1980] Bass, N.M., Connolly, J.J. 1980 The Performance of Industrial Platinum Resistance Thermometers; *Aust. J. Instrumentation and Control* 36, 88-90
- [Batagelj 2003] Batagelj, V. Bojkovski, J., Drnovsek, J. 2003 Methods of reducing the uncertainty of the self-heating correction of a standard platinum resistance thermometer in temperature measurements of the highest accuracy, *Meas. Sci. Technol.* 14, 2151
- [Benedict 1963] Benedict, R.P., Murdock, J.W., 1963 *ASME Trans. J. Eng. Power* 235
- [Bentley 1998] J.J. Connolly and E. Corina Horrigan, *Handbook of Temperature Measurement Vol. 2: Resistance and Liquid-in-Glass Thermometry*, Ed. R.E. Bentley, Springer Science & Business Media, 1998, ISBN 9789814021104
- [Besley 1983] Besley, L.M., Kemp, R.C., 1983 The Use of Industrial Grade Platinum Resistance Thermometers between 77 K and 273 K; *Cryogenics* 23, 26-28
- [Berry 1982] Berry, J., 1982a Evaluation and Control of Platinum Oxidation Errors in Standard Platinum Resistance Thermometers; *Temperature: Its*

- Measurement and Control in Science and Industry (American Institute of Physics, New York) 5, 743-752
- [Berry 1982b] Berry, J., 1982b Oxidation, Stability, and Insulation Characteristics of Rosemount Standard Platinum Resistance Thermometers; Temperature, Its Measurement and Control in Science and Industry (American Institute of Physics, New York) 5, 753-762
- [Boguhn 2011] Boguhn, D., Koepke, M., 2011 Typical R(T90) Characteristics of Platinum Thin-Film Resistance Thermometers in the Temperature Range from -50 °C to +660 °C, *Int. J. Thermophys.* **32** 2379-2387
- [Bosma 2013] Bosma, R., de Bruin-Barendregt, C.K., van Breugel, A., Peruzzi, A., 2013 A low Temperature Comparator for Calibration of Industrial Thermometers in the Range -190 °C to -25 °C, *Temperature: Its Measurement and Control in Science and Industry, Volume 8, AIP Conf. Proc.* 1552, 480-485; doi: 10.1063/1.4819588
- [Bugbee 1996] Bugbee, B., Monje, O., Tanner, B., 1996 Quantifying energy and mass transfer in crop canopies, *Adv. Space Res.* 18, 149–56
- [CCT/03-14] Report of Working Group 2 to the Comité Consultatif de Thermométrie: April 2003
- [Chattle 1975] Chattle, M.V., 1975 Resistance Ratio/Temperature Relationships for Industrial Platinum Resistance Thermometers; NPL Report QU 30
- [Chattle 1977] Chattle, M.V., 1977 Resistance Ratio/Temperature Relationships for Industrial Platinum Resistance Thermometers of Thick Film Construction; NPL Report QU 42
- [Childs 2001] Childs P.R.N., 2001 Practical Temperature Measurement, Butterworth-Heinemann 2001, ISBN 978-0750650809
- [Cimerman 1999] Cimerman, F., Glagojević, B., Bajsić, I., 1999 Step input response of Pt100 film resistance temperature sensors, *Proceedings TEMPMEKO '99* (editors Jaco F. Dubbeldam and Martin J. de Groot), Delft, Nmi-VSL, pp. 347-352
- [Cochrane 1972] Cochrane, J., 1972 Relationship of the Chemical Composition to the Electrical Properties of Platinum; in *Temperature, Its Measurement and Control in Science and Industry*, edited by H. H. Plumb, (Instrument Society of America, Pittsburgh) 4, 1619-1632
- [Connolly 1982] Connolly, J.J., 1982 The Calibration Characteristics of Industrial Platinum Resistance Thermometers; *Temperature: Its Measurement and Control in Science and Industry* (American Institute of Physics, New York) 5, 815-817
- [Connolly 1992] Connolly, J.J., 1992 Interpolation equations for industrial platinum resistance thermometers; *Temperature: Its Measurement and Control in Science and Industry* (American Institute of Physics, New York) 6, 419-422
- [Crovini 1992] Crovini L., Actis, A., Coggiola, G., Mangano, A., 1992 Precision calibration of Industrial Platinum Resistance Thermometers; *Temperature: Its Measurement and Control in Science and Industry* (American Institute of Physics, New York) 6, 1077-1082

- [Curtis 1982] Curtis, D.J., 1982 Thermal Hysteresis and Stress Effects in Platinum Resistance Thermometers; *Temperature: Its Measurement and Control in Science and Industry* (American Institute of Physics, New York) 5, 803-812
- [Davis 2001] Davis, J.R., 2001 *Alloying – Understanding the Basics*, ASM International (2001) ISBN 978-0-87170-744-4
- [De Podesta 2018] de Podesta, M., Bell, S., Underwood, R., 2018 Air temperature sensors: dependence of radiative errors on sensor diameter in precision metrology and meteorology, *Metrologia* 55 229 (2018)
- [Dubbeldam 1998] Dubbeldam, J.F., de Groot, M.J., 1998 in *EUROMET Workshop in Temperature* (BNM/CNAM, Paris, 1998), pp. 39-44
- [Fericola 2008] Fericola, V.C., Iacomini, L., 2008 Approximating the ITS-90 temperature scale with industrial platinum resistance thermometers; *Int. J. Thermophys.* 29, pp. 1817-1827
- [Gam 2011] Gam, K.S., Yang, I., Kim, Y.-G., 2011 Thermal Hysteresis in Thin-Film Platinum Resistance Thermometers, *Int. J. Thermophys.* 32, 2388-2396
- [Hahtela 2014] Hahtela, O., Heinonen, M., Kajastie, H., Ojanen, M., Riski, K., Strnad, R., 2014 Calibration of Industrial Platinum Resistance Thermometers up to 700 °C, *Int. J. Thermophys.* 35, 668-680
- [Hamon 1954] Hamon, B.V., 1954 A 1-100 Ω build-up resistor for the calibration of standard resistors. *J. Sci. Instrum.* 35, 450–453
- [Harrison 2015] Harrison, R.G., 2015 *Meteorological Measurements and Instrumentation*, Wiley, New York
- [Hashemian 1990] Hashemian, H.M., Beverly, D.D., Mitchell, D.W., Petersen, K.M., 1990 Aging of Nuclear Plant Resistance Temperature Detectors, US Nuclear Regulatory Commission, Report No. NUREG/CR-5560, 181 pp.
- [Hashemian 1992] Hashemian, H.M., Petersen, K.M., 1992 Achievable accuracy and stability of industrial RTDs; *Temperature: its Measurement and Control in Science and Industry* (American Institute of Physics, New York) 6, 427-432
- [Hill 2008] Hill, K.D., 2008 Investigating the Behaviour of Industrial Platinum Resistance Thermometers from 13.8 K to 273.16 K, *Acta Metrol. Sin.* 12, 55
- [IEC 60751] IEC 60751:2008 Industrial platinum resistance thermometers and platinum temperature sensors, International Electrotechnical Commission, Geneva
- [IEC 62397] IEC 62397:2007 Nuclear power plants – Instrumentation and control important to safety – Resistance temperature detectors, International Electrotechnical Commission, Geneva
- [JIS 1981] JIS C 1604, 1981 Platinum Resistance thermometers, Japanese Standards Association, Tokyo
- [Jursic 2014] Jursic I., Rudtsch, S., 2014 Thermal Stability of β -PtO₂ Investigated by Simultaneous Thermal Analysis and Its Influence on Platinum Resistance Thermometry, *Int. J. Thermophys.* 35 1055-1066 DOI 10.1007/s10765-014-1695-0

- [Kaiser 1999] Kaiser, N.E., 1999 Accurate temperature measurements using Pt100 resistance thermometers, Proceedings TEMPMEKO '99, (editors Jaco F. Dubbeldam and Martin J. de Groot), Delft, Nmi-VSL, pp. 365-370
- [Kerlin 1982] Kerlin, T.W., Shepard, R.L., Hashemian, H.M., Petersen, K.M., 1982 Response of Installed Temperature Sensors; Temperature: Its Measurement and Control in Science and Industry (American Institute of Physics, New York) 5, 1357-1366
- [Kretz 2013] Kretz, A., Krogmann, F., 2013 Platinum Thin-film Sensors for Space, Proceedings of the Space Passive Components Days, 1st International Symposium, 24-26 September 2013 ESA-ESTEC (The Netherlands) European Space Components Information Exchange System, <https://escies.org/download/webDocumentFile?id=60970>
- [Liptak 2003] Liptak, B.G. (editor in chief), 2003 Instrument Engineer's Handbook, 4th Ed., Vol. 1 Process Measurement and Analysis Chapter 4. Temperature Measurement, CRC Press, pp 561-708
- [Ljungblad 2013] Ljungblad, S., Holmsten, M., Josefson, L.-E., Klevedal, B., 2013 Long Term Stability and Hysteresis Effects in Pt100 Sensors Used in Industry, Temperature: Its Measurement and Control in Science and Industry, Volume 8, AIP Conf. Proc. 1552, 421-426 doi: 10.1063/1.4819578
- [Mangum 1982] Mangum, B.W., Evans, G.A., 1982 Investigation of the Stability of Small Platinum Resistance Thermometers; Temperature: Its Measurement and Control in Science and Industry (American Institute of Physics, New York) 5, 795-801
- [Mangum 1984] Mangum, B.W., 1984 Stability of Small Industrial Platinum Resistance Thermometers; J. Research Nat. Bur. Stand. 89, 305-316
- [Marcarino 1999] Marcarino P., Steur P. P. M., Dematteis R., 1999 Calibration of SPRTs, affected by humidity, in the sub-range between the fixed points of Hg and Ga, Proc. Proceedings TEMPMEKO '99, (editors Jaco F. Dubbeldam and Martin J. de Groot), Delft, Nmi-VSL, pp. 80-83
- [Marcarino 2001] Marcarino, P., Steur, P.P.M., Bongiovanni, G., Cavigioli, B., 2001 ITS-90 approximation by means of non-standard platinum resistance thermometers, Proceedings TEMPMEKO 2001 (editors B. Fellmuth, J. Seidel, G. Scholz), VDE VERLAG GMBH, Berlin, pp. 85-90
- [Marcarino 2004] Marcarino P., Steur P.P.M., Merlone A., 2004 Interpolation for industrial platinum resistance thermometers; Advanced Mathematical and Computational Tools in Metrology VI, Edited by P. Ciarlini, M.G. Cox and G.B. Rossi, World Scientific Publishing Company, pp. 318-322
- [Marcarino 2004b] Marcarino, P., Merlone, A., Steur, P.P.M., Actis, A., Antinori, M., 2004 Proposal: New reference functions for industrial platinum resistance thermometers, Proc. 9th International Symposium on Temperature and Thermal Measurements in Industry and Science (Tempmeko 2004), 807-812 (2004)
- [Mendez-Lango 2001] Méndez-Lango, E., Ramirez-Bazán, R., 2001 Calibration of industrial grade platinum resistance thermometers by ITS-90 fixed points,

- Proceedings TEMPMEKO 2001 (editors B. Fellmuth, J. Seidel, G. Scholz), VDE VERLAG GMBH, Berlin, pp. 647-651
- [Michalski 2001] Michalski, L., Eckersdorf, K., Kucharski, J., McGhee, J., 2001 Temperature Measurement, John Wiley & Sons, ISBN 978-0471867791
- [Moiseeva 2002] Moiseeva, N.P., 2002 Investigation of $W(T_{90})$ functions for low- α PRTs in the sub-ranges above 0 °C; Proceedings of Temperature: Its Measurement and Control in Science and Industry, Vol. 7, edited by Dean C. Ripple, Chicago, American Institute of Physics, 2003, 333-338
- [Murdock 2009] Murdock, W.E., Strouse, G.F., 2009 NIST Determination of Industrial Platinum Resistance Thermometer Hysteresis from -196 °C to 200 °C, NCSLI Meas. **5**, 28
- [Nicholas 2001] Nicholas, J.V., White, D.R., 2001 Traceable Temperatures, J Wiley & Sons Ltd, Chichester, UK, Second edition
- [OIML R 84] International Recommendation OIML R 84 Edition 2003 (E), Platinum, copper and nickel resistance thermometers (for industrial and commercial use), International Organization of Legal Metrology
- [Pearce 2013] Pearce, J.V., Rusby, R.L., Harris, P.M. Wright, L., 2013 The optimization of self-heating corrections in resistance thermometry, Metrologia 50, 345-353
- [Pearce 2016] Pearce, J.V., Gray, J., Veltcheva, R.I., 2016 Characterisation of a Selection of AC and DC Resistance Bridges for Standard Platinum Resistance Thermometry, Int. J. Thermophys. **37**, 109
- [Quinn 1990] Quinn, T.J., 1990 Temperature, Academic Press, 2nd Edition, 1990, ISBN 9781483259345
- [Rhys 1969] Rhys D.W., Taimsalu, P., 1969 Effect of Alloying Additions on the Thermoelectric Properties of Platinum, Engelhard Industries Technical Bulletin, 10, 41-47
- [Rudtsch 2020] Rudtsch S., unpublished
- [Rusby 2017] Rusby R.L., Machin, D. 2017 Hysteresis and Instability in Some IPRT Sensors Within Temperature Ranges Extending from -196 °C to 150 °C, Int. J. Thermophys. **38**, 117
- [Sakurai 1996] Sakurai, H. Mizuma, Y., Hamada, T., Suyama, Y., 1996 Reference function for JPt100 thermometers based on the ITS-90, Transactions of the Society of Instrument and Control Engineers, Vol. 32, Issue 8 pp.1139-1144.
- [Sato 2013] Sato, H., 2013 Stability Test of Industrial Platinum Resistance Thermometers at 450 °C for 1000 hours, Temperature: Its Measurement and Control in Science and Industry, Volume 8, AIP Conf. Proc. 1552, 417-420 (2013); DOI: 10.1063/1.4819577
- [Sinclair 1972] Sinclair, D.H., Terbeek, H.G., Malone, J.H., 1972 Calibration of Platinum Resistance Thermometers; Temperature: Its Measurement and Control in Science and Industry (Instrument Society of America, Pittsburgh 4, 983-988

- [Strouse 2008] Strouse, G.F., 2008 Standard Platinum Resistance Thermometer Calibrations from the Ar TP to the AG TP, NIST Special Publication 250-81
- [Tamura 1992] Tamura, O., Sakurai, H., Nakajima, T., 1992 Low-temperature characteristics of some industrial-grade platinum resistance thermometers; *Temperature: Its Measurement and Control in Science and Industry* (American Institute of Physics, New York) 6, 443-448
- [Veltcheva 2013] Veltcheva, R.I., Pearce, J.V., da Silva, R., Machin, G., Rusby, R.L., 2013 Strategies for minimizing the uncertainty of the SPRT self-heating correction, 9th International Temperature Symposium, Los Angeles, *Temperature: Its Measurement and Control in Science and Industry*, vol. 8, ed. by C.W. Meyer, AIP Proceedings 1552 (AIP, Melville, NY, 2013), pp. 433-438
- [Veltcheva 2018] Veltcheva, R.I., Rusby, R.L., Peters, D.M., Watkins, R.E.J., 2018 Experiences in Calibrating Industrial Platinum Resistance Sensors Between $-196\text{ }^{\circ}\text{C}$ and $80\text{ }^{\circ}\text{C}$, *Int. J. Thermophys.* 39:65
- [Veltcheva 2020] Veltcheva R.I., Pearce, J.V., 2020 private communication
- [Vines 1941] Vines, R.F., Wise, E.M., 1941 *The Platinum Metals and Their Alloys*, The International Nickel Company, Inc., New York
- [White 1997] White, D.R., Williams, J.M., 1997 A resistance network for verifying the accuracy of resistance bridges. *IEEE Trans. Instrum. Meas.* 46, 329–332
- [White 2007] White, D.R., Saunders, P., 2007 The propagation of uncertainty with calibration equations, *Meas. Sci. Technol.* **18** 2157 (2007)
- [White 2008] White, D.R., Clarkson, M.T., Saunders, P., Yoon, H., 2008 A general technique for calibrating indicating instruments, *Metrologia* **45**, 199–210
- [White 2010] White, D.R., Jongenelen, C.L., Saunders, P., 2010 The Hysteresis Characteristics of Some Industrial PRTs, *Int. J. Thermophys.* **31**, 1676-1684
- [White 2010b] White, D.R., and Jongenelen, C.L., The Immersion Characteristics of Industrial PRTs, *Int. J. Thermophys.* **31**, 1685-1695 (2010)
- [White 2013] White, D.R., Edgar, H., McLennan, B.E., Saunders, P., 2013 Automation of the resistance bridge calibrator. *AIP Conf. Proc.* 1552, 392
- [White 2017] White, D.R., 2017 MSL Technical Guide 18: Resistance Measurement for Thermometry, Version 2, December 2017 (Measurement Standards Laboratory of New Zealand)
- [Yamazawa 2011] Yamazawa, K., Anso, K., Widiatmo, J.V., Tambo J., Arai, M., 2011 Evaluation of Small-Sized Platinum Resistance Thermometers with ITS-90 Characteristics; *Int. J. Thermophys.* 32 2397-2408
- [Yang 2015] Yang, I., Suherlan, Gam, K.S., Kim, Y.-G., 2015 Interpolating equation of industrial platinum resistance thermometers in the temperature range between $0\text{ }^{\circ}\text{C}$ and $500\text{ }^{\circ}\text{C}$, *Meas. Sci. Technol.* **26**, 035104
- [Zhang 1992] Zhang Jipei, Fan Kai, Wu Shuyuan and Yao Quanfa, 1992 Investigation on the R-T relationship above $0\text{ }^{\circ}\text{C}$ and the stability of industrial

platinum resistance thermometers; *Temperature: Its Measurement and Control in Science and Industry* (American Institute of Physics, New York) **6**, 433-438

[Zhang 1997] Zhang, J., Nagao, Y., Kuwano, S., Ito, Y., 1997 Microstructure and Temperature Coefficient of Resistance of Platinum Films, *Jpn. J. Appl. Phys.* **36**, 834-839

[Zuzek 2010] Žužek, V., Batagelj, V., Bojkovski, J., 2010 Determination of PRT Hysteresis in the Temperature Range from -50 °C to 300 °C, *Int. J. Thermophys.* **31** 1771-1778

[Zvizdic 2013] Zvizdić D., Šestan, D., 2013 Hysteresis of thin film IPRTs in the Range 100 °C to 600 °C, *Temperature: Its Measurement and Control in Science and Industry*, Volume 8, AIP Conf. Proc. 1552, 445-450 doi: 10.1063/1.4819582